

TUNNEL FACE STABILITY

*Collapse mechanisms, design
and construction principles*



DISCLAIMER

The purpose of the information documents is to provide information on a new or insufficiently covered technique or problem. The reader may find it useful in his or her work. The content and any conclusions presented should not be considered as recommendations by the CETU. Although every effort has been made to ensure the reliability of the sources used, neither CETU nor the authors of the document can be held responsible.

TUNNEL FACE STABILITY

*Collapse mechanisms, design
and construction principles*

December 2022

Centre d'Études des Tunnels (Centre for Tunnel Studies)

25 Avenue François Mitterrand

69500, Bron, France

Tel. +33 (0)4 72 14 34 00

Fax. +33 (0)4 72 14 34 30

cetu@developpement-durable.gouv.fr

www.cetu.developpement-durable.gouv.fr

TABLE OF CONTENTS

1 CONTEXT AND PURPOSE OF THIS DOCUMENT	5
2 GENERAL PRINCIPLES FOR STABILITY STUDIES	7
2.1 Problem statement	7
2.2 Hypothesis and notations	8
2.3 Calculation configurations	9
2.4 Safety factor approach	10
2.5 Modelling approaches	11
3 ASSESSMENT OF STABILITY CONDITIONS	13
3.1 Discontinuous medium	13
3.2 Continuous undrained medium	14
3.3 Continuous drained medium without seepage	17
3.4 Continuous drained medium with seepage	22
4 ON-SITE OBSERVATIONS AND CONSTRUCTION MEASURES	26
4.1 Construction methods in conventional tunnelling	26
4.2 Monitoring methods in conventional tunnelling	28
4.3 Construction methods in conventional tunnelling	28
4.4 Monitoring methods for pressurized face tunnelling	29
5 SUMMARY	30
6 GLOSSARY	32
7 REFERENCES	33
8 APPENDIX: FACE STABILITY EXAMPLES	36

CONTEXT AND PURPOSE OF THIS DOCUMENT

The tunnel face exerts its immediate influence on the “active” zone of tunnelling in front of and behind the face (AFTES WG16, 2020). Pushed back as the tunnelling process advances, the majority of shifts in ground stresses occur in this zone.

For deep tunnels, stress redistribution (which may or may not require interventions at the face, depending on the quality of the ground), enhances the formation of the arch, which helps to restore the overall balance throughout the zone. For shallow tunnels, these arching effects are obtained with greater difficulty and stresses that are not correctly dealt with can give rise to surface settlements, causing damage to neighbouring structures. The considerable deformation of poor ground at great depth can lead to a decompressed zone at the edge of the excavation area. Gravity-related phenomena can occur in this decompressed zone as well as near the surface.

Numerous instabilities have already been observed in different geotechnical contexts. CEDD (2015) draw up, for example, a (non-exhaustive) list of more than sixty instabilities that appeared between 1977 and 2014, at the face or at the wall. The sheets available in the appendix provide some additional, fairly recent examples. The following findings result from these examples:

- face instabilities are possible in a wide variety of geotechnical contexts (homogeneous or mixed faces, fractured rockmass, soft grounds, etc.), and for all boring methods (conventional tunnelling, open face shield, earth pressure balance or slurry shield),
- underground, the volumes involved can range from a few cubic decimetres for localized instabilities to several hundred cubic metres for global instabilities affecting the entire front or even the overburden,
- the shape of the mechanisms depends on the nature of the ground: blocks delimited by the pre-existing discontinuities in rocks, mechanisms localized near the face in powdery grounds (with regressive evolution towards the surface) and more voluminous mechanisms in cohesive clayey grounds,
- instabilities induced by partial or inappropriate control of the face stability can progress to the surface with a delayed effect in time and space,
- the consequences of face instabilities are very variable, ranging from being “almost negligible” to “very significant” with delays (up to several months) or significant additional costs (up to several million euros), and casualties (as underground workers are exposed to risks).

Consequently, a good understanding of the mechanisms by which the ground is deformed is necessary in order to avoid initiating collapse mechanisms or to predict the consequences when they can not be avoided. This understanding will:

- ensure the safety of the site (primarily that of underground workers) and its surroundings (especially neighbouring structures on the surface),
- allow the installation of pre-support structures at the front and support structures at the back of the working face,
- help the project comply with time and budget requirements by limiting overbreaks and avoiding a situation with unpredicted and uncontrolled stresses,
- contribute to the long term stability of the construction, by limiting deterioration of the surrounding ground at the edge of the excavation zone and therefore the stresses on the final lining structures.

The aim of this information document is to provide a general overview of failure mechanisms, available modelling approaches and their scope of application, as well as suitable calculation tools for each project. Indeed, this topic has not yet been the subject of a standard (Eurocode 7 standard for example) nor a French (AFTES) or international (ITA-AITES) design recommendation. The document that comes closest is the recommendation from the DAUB (German counterpart of the AFTES) published in 2016, but which remains specific to the case of TBMs and introduces elements specific to the German context.

The present document is mainly intended for engineers in design offices, project managers and contractors. By providing a summary of a broad literature review, the various instability mechanisms are presented and structured according to the nature of the ground (rockmass with varying degrees of fracturing, loose ground such as gravelly soil or fine soil, etc.) and the excavation method (conventional method with or without reinforcement of the face or pre-support, pressurised or unpressurised TBM). It can also be useful to engineers in charge of monitoring the works (support manager on the contractor’s side, geotechnical supervision on the project manager’s side) in order to understand the behaviour of the ground during excavation, then choose and adapt the best construction measures in response to the encountered mechanisms.

For each configuration, the different methods for calculating face stability are described and an explicit empirical formulation for “operational” purposes is proposed. This document aims to be easily usable by engineers by giving an overview of the different existing methods and their field of application.

This document does not address the essential issue of the choice of calculation parameters, in particular the shear strength parameters of the ground. In accordance with Eurocode 7-1 (AFNOR, 2005), this choice must be based on the measured values, values obtained from on-site tests and laboratory tests, supplemented by the lessons learned from experience. For stability issues, estimates need to be cautious, in particular as regards effective cohesion. In case of significant uncertainty, calculations must be carried out to provide values within various ranges.

If studies highlight unstable conditions at the face or if instability is encountered during the works, different construction processes can be used to improve the stability of the face or work safety. The main methods used in both conventional and mechanized tunnelling are thus outlined, as well as necessary monitoring actions during works, in order to confirm the geotechnical assumptions made during the studies and to determine the actual stability conditions.

GENERAL PRINCIPLES FOR STABILITY STUDIES

2.1 PROBLEM STATEMENT

Consider the ideal case of a tunnel perfectly supported in its interior zone, with only the face free to move and on which a certain pressure is exerted (which can be zero in the case of an unsupported face).

In the case of a TBM with a pressurized face, this pressure is actually exerted by compressed air (air pressure), excavated material (earth pressure) or bentonite (slurry pressure, with conventional or "heavy" slurry). In conventional tunnelling, an "equivalent" confinement pressure can be considered to take into account face bolting.

Depending on the extent of this pressure, extrusion movements (towards the tunnel cavity) or upheaval movements (towards the front of the face when viewed from inside the tunnel in the advancement direction) may occur. Their amplitude notably depends on the geometry of the tunnel, the initial state of stresses and the geotechnical characteristics of the ground.

Figure 1 gives a schematic view and also makes the link with surface movements in the case of a shallow tunnel above the water table:

- if the pressure exerted on the face is less than the horizontal geostatic stress ($\sigma_T < \sigma_{h0}$), an extrusion movement of the face appears and may lead to surface settlements. The face may collapse with the appearance of a sinkhole for extreme cases,
- on the other hand, if the pressure exerted on the face is greater than the horizontal geostatic stress ($\sigma_T > \sigma_{h0}$), an upheaval movement of the tunnel face appears, and can lead to a surface upheaval in front of the face (this case, however, is only possible with an earth pressure balance tunnel boring machine under a very low overburden).

In a global approach to evaluate the acceptable range of pressure within the scope of a tunnelling project, a stability range (shown in red in Figure 1) is evaluated, which prevents the occurrence of failure mechanisms by collapse or blow-out. In addition, the evaluation of a range of "admissible displacements" (in green in Figure 1) is needed for shallow tunnels, depending on the sensitivity of neighbouring constructions.

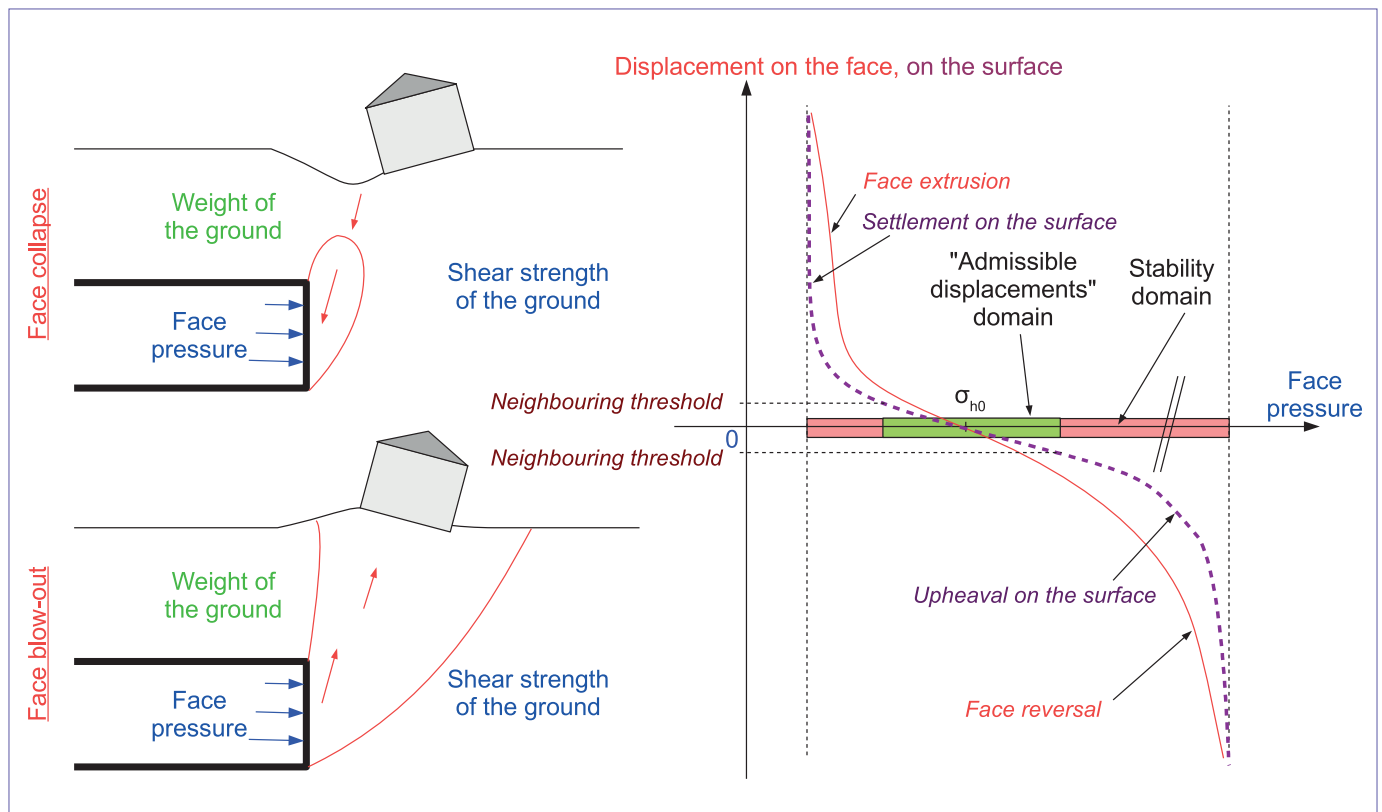


Figure 1: Links between face pressure, instability mechanisms at the face and displacements generated in proximity to neighbouring structures in the case of a shallow tunnel.

If the air, earth or slurry pressure at the face do not counteract pore pressures in the ground, two related effects may occur: (i) seepage forces that increase the instability of the face, and (ii) potentially large volumes of water that can lead to the flooding of the works site.

This information document is mainly devoted to the lower limit of the stability range, i.e. the minimum pressure to be exerted to prevent collapse.

The lower limit of the “acceptable” range with respect to the sensitivity of any neighbouring structures in the case of a shallow tunnel is based on semi-empirical approaches (so-called “volume loss” method) or numerical calculations. This point is not addressed

here as it is an issue in its own right. The recommendations of AFTES WG16 (2020) provide information on this subject: evaluation of the intrinsic sensitivity of neighbouring constructions, evaluation of the displacements induced by underground works and evaluation of the associated level of damage.

The case of face pressures higher than the existing horizontal stresses is easier to deal with from an operational point of view. Indeed, the theoretical approaches (limit equilibrium or yield design theory) dedicated to face blow-out imply a total mobilization of the shear stresses along the collapsed surfaces, which always leads to maximum face pressures much higher than those leading to significant upheaval movements on the surface (Berthoz et al., 2012).

2.2 HYPOTHESIS AND NOTATIONS

The study of face stability is usually based on the following assumptions with the notations summarised in Figure 2:

- **Geometry:** The face is equated to a disc with a diameter D . In conventional tunnelling, the actual excavation is not circular and a disc, (or even a rectangle), equivalent to the area covered by the face is generally used. If the excavation is very narrow (horizontally or vertically), the choice may be more difficult, and is to be made with regard to the geometry of the mechanism involved. In addition, C is the overburden thickness, H is the depth of the tunnel axis, and d is the length of the unsupported span (area not supported during excavation).
- **Hydrogeology:** We consider the groundwater table to be located at a height H_w above the tunnel axis. In the case of a confined aquifer, an equivalent height H_w deduced from the hydrostatic pressures can be estimated in order to include it in the same case study.
- **Geology and geotechnical engineering:** the face, whether homogeneous or composed of different facies, may comprise:
 - “mildly fractured” rockmass with few discontinuities at the scale of the face, and behaving as discontinuous media at the scale of the construction. In this case, the stability is conditioned by the density γ of the unstable dihedra, the orientation of the discontinuities θ and the shear strength along the discontinuities, in particular the friction angle φ'_{disc} ,
 - “loose” ground (soils, highly fractured rocks), which can be considered as continuous at the scale of the construction, or as intact rock, continuous by definition. In this case, each facies is generally assimilated to a homogeneous medium of density γ , of permeability k , of perfectly plastic rigid behaviour parametrised by a Mohr-Coulomb criterion (c' , φ') under drained conditions, Tresca (C_u) under non-drained conditions, or possibly Hoek & Brown for rocky soils.
- **Surface load:** σ_s denotes the constant pressure exerted at the surface, so as to simulate the weight of the buildings on the surface (considering 12 kPa per building floor for example), excess site loads (generally around 20 kPa) or excess operating loads (around 10 kPa for a roadway for example).

- **Excavation method and confinement pressure:**

- Excavation can be carried out with a TBM or by conventional tunnelling. In both cases, the average advancement rate of the face (integrating the excavation and support phases) is noted v_{avct}
- a constant pressure σ_T is considered in order to represent the boundary conditions on the surface of the face and along the unsupported span. In practice, we consider the value exerted in the tunnel axis. For tunnels with very large diameters (greater than about ten meters), it is important to take into account the face pressure gradient over the height of the face, or at least, ensure that the pressure retained in the axis is representative of the real boring conditions.

The minimum value of this pressure σ_T is calculated so that the stability of the face is ensured. If this value is negative (with the sign conventions of soil and rock mechanics, i.e. positive stresses in compression), the face is considered theoretically self-stable. If it is positive, the face is not self-stable and suitable construction processes must be implemented to ensure stability. These processes are designed on the basis of this pressure value with a safety margin to be defined.

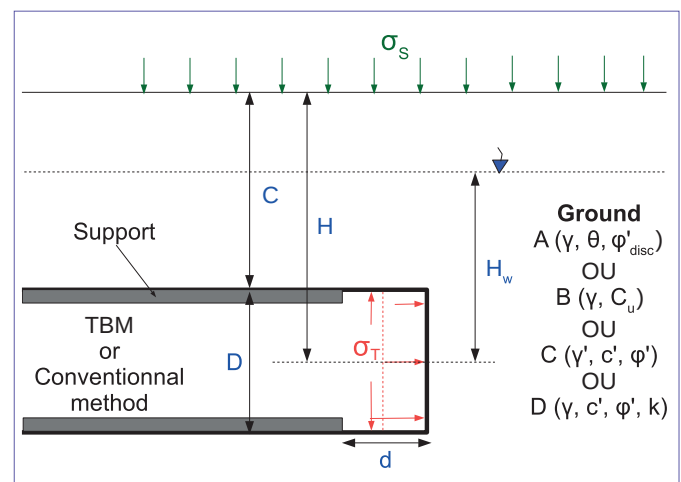


Figure 2: Problem position and notations.

2.3 CALCULATION CONFIGURATIONS

Different calculation configurations are derived from the previous assumptions. These four cases are detailed in chapter 3.

CASE A Discontinuous medium

In mildly fractured rockmasses, the network of discontinuities cuts potentially unstable dihedrals. Blocks falls or slides can appear at the face and/or in the unsupported span area. The geometry of the dihedra that may become detached depends on the geometry of the face and the orientation of the main families of discontinuities. Without support, the stability of these dihedra depends on their geometry, on the density of the rock matrix and on the shear strength which can be mobilised on the discontinuities surfaces.

In rocky grounds with little overall fracturing, more fractured zones or fault zones with degraded, altered materials may exist, in which it may be relevant to retain mechanisms of type B/C/D below.

CASE B Continuous undrained medium

In the case of TBM or conventional tunnelling progressing at a high speed in ground with low permeability, it may be reasonable to consider that excavation is carried out under “undrained” conditions.

In this context, the calculation is carried out in total stresses with the total density γ of the ground and the undrained shear strength of the ground (parametrized by an “undrained cohesion” C_u , and a zero friction angle ϕ_u). The solution to the problem (minimum face pressure preventing face collapse σ_{T-eff}) is written as follows:

$$\sigma_{T-eff} = f_1(\gamma, D, H, \sigma_s, C_u) \quad [1]$$

The choice between “undrained” and “drained” conditions must be considered specifically for each geotechnical context and each actual construction phase. Based on hydro-mechanical calculations, Anagnostou & Kovari (1996) give the following limit to this calculation case: permeability k less than 10^{-7} to 10^{-6} m/s and penetration advance speed v_{avct} greater than 0.1 to 1 m/h. It is important to take into account any stoppages in excavation works (due to hyperbaric operations, weekends, site incidents...), as by slowing the advancement of the face, these stoppages may mean that the “undrained” assumption is unrealistic. If there is any doubt about the reality of undrained conditions, both calculations (drained and undrained) can be carried out to judge the sensitivity of the face stability conditions with regard to this assumption.

CASE C Continuous drained medium without seepage

In the case of more permeable ground or slower boring (with the above example values, $k > 10^{-6}$ m/s and $v_{avct} < 0.1$ m/h), the ground is solicited in a “drained” state (*i.e.* without pore overpressures). In this case, the stability of the face is conditioned by the effective stresses exerted in the ground.

There is no seepage of pore water into the ground (water pressures remain equal to the initial hydrostatic pressures) in the following cases:

- boring outside the water table, naturally, or induced by the work (preliminary water table lowering, drainage while advancing leading to the absence of hydrostatic pressures up to at least one diameter in front of the face),
- pressurized TBM tunnelling under the water table in relatively coarse soils, apart from uncontrolled conditions corresponding to the “drained with seepage” case.

The face pressure to be exerted is then the sum of the pressure exerted by the ground (calculated as effective stresses, with the assumption of a shear strength isotropy) and the (hydrostatic) pressure of the water, *i.e.*:

$$\sigma_{T-eff} = \max(\sigma'_{T-eff}; 0) + u = f_2(\gamma', D, H, \sigma_s, c', \phi') + \gamma_w \cdot H_w \quad [2]$$

Outside the water table, the effective stresses are equal to the total stresses and the solution is reduced to:

$$\sigma_{T-eff} = f_2(\gamma, D, H, \sigma_s, c', \phi') \quad [3]$$

CASE D Continuous drained medium with seepage

In conventional tunnelling (or possibly with an open face TBM) below the water table, the hydraulic imbalance between the inside of the tunnel (zero pressure) and the ground (initial pore pressure equal to the hydrostatic pressure) leads to seepage directed towards the face.

With a pressurized face TBM below the water table, the seepage towards the face is prevented: (a) due to the low permeability of the cake, control of the mucking rate and control of the air bubble pressure in the crown of the working chamber with a slurry pressure balance shield TBM, (b) thanks to the right sizing of the screw conveyor (length and diameter) coupled with the addition of possible admixtures reducing permeability in the working chamber with an earth pressure balance shield TBM. Pore overpressures can be generated at the face if these conditions are insufficiently controlled.

In all of these conditions, the distribution of pore pressures (thus also of effective stresses) depends on the conditions at the hydraulic boundaries of the model (function of H_w) and on the ground permeability (k). The pressure to be exerted on the face to ensure its stability then depends on the seepage forces. In steady state, these depend only on the hydraulic gradient (function of H_w and k). In transient conditions, time (t)

is also a factor, and the duration after which the face becomes unstable can be assessed. The general shape of the minimum pressure preventing face collapse is therefore as follows:

$$\sigma_{T-eff} = f_3(\gamma', D, H, \sigma_s, c', \varphi', H_w, k, t) \quad [4]$$

2.4 SAFETY FACTOR APPROACH

Three main approaches are possible in absolute terms:

- with partial safety coefficients on the effects of the actions: in this case, the calculations are carried out without safety coefficients, then the forces obtained related to the stability of the ground (or the stresses σ_{T-eff} if the face is homogeneous and totally below the water table) and to the water pressure are multiplied by safety coefficients,
- with partial safety coefficients applied before calculation, directly on the ground shear strength parameters,
- by seeking an overall safety coefficient, thanks to the calculation of the ratio between the driving forces and the resisting forces without weighting the ground parameters or the effects of the actions.

As “category 3 geotechnical structures” (§2.1 of Eurocode 7-1), tunnels are currently outside the scope of Eurocode 7, however the approaches used in practice are compatible with its principles. For the design of tunnel support and lining structures using “displacement” approaches (finite element type), AFTES has taken a position by recommending the weighting of the effects of actions: normal forces and bending moments in the structures (AFTES WG29, 2007). This choice is motivated by the desire not to induce plastic behaviour by taking into account degraded parameters for the ground, which would be likely to artificially disturb the distribution of forces between the ground and the lining.

For the study of face stability in a poorly fractured rock mass (dihedral falls and slides) by “failure” methods (limit equilibrium and yield design methods), a “global safety factor” type approach is recommended. Indeed, a degradation of the rock mass parameters (level of fracturing, state of alteration, shear strength on discontinuities, etc.) could lead to a significant modification of the geometry of the blocks, or even to a radical modification of the mechanisms in play, the ground being able to pass from a behaviour of discontinuous medium type to that of a continuous medium. By analogy with radial bolting in the interior zone (AFTES WG30, 2021), an overall safety factor of the order of 1.6 to 1.8 can be sought at the face, for example.

In soft ground, the German recommendation (DAUB, 2016), which deals more specifically with pressurised TBMs, recommends weighting the effects of the actions, with partial safety factors of 1.5 on the earth pressure σ_{T-eff} and 1.05 on the water pressure. This approach may be relevant when $\sigma_{T-eff} \gg 0$, but is questionable when the face is at the limit of stability, the condition $\sigma_{T-eff} = 0$ being true regardless of the safety coefficient considered.

By analogy with the problems of slope stability, an overall safety factor can be estimated by relating the driving forces to the resisting forces. A calculation approach with partial coefficients on the resistance of the ground can also be considered in soft ground (Paternesi et al., 2017) since the degradation of the ground parameters (in particular the friction angle) increases the geometry of the mechanism but does not change the overall behaviour, which remains a continuous medium. This is the approach adopted in this document for soft ground with the following partial safety coefficients:

- 1.25 on c' and $\tan(\varphi')$ in drained conditions,
- 1.4 on C_u in undrained conditions.

In the case of pressurised TBM excavation, the calculated minimum pressures σ_T can be increased by 10 kPa in the case of a slurry shield (SS) and 30 kPa in the case of an earth pressure balanced shield (EPB) in order to take into account the difficulties in maintaining and controlling the applied face pressure (DAUB, 2016). It is also reasonable to increase the water pressures by 5% in the case of a continuous drained medium without flow (Case C, §.2.3).

However, the recommended approach of applying a partial weighting on the shear strength parameters in soft ground is clearly not recommended for the design of support and lining structures, due to the modification of the soil/structure interaction phenomena.

2.5 MODELLING APPROACHES

All the existing models for studying the stability of the working face can be grouped into four main categories, the main principles of which are given below, with some examples in Illustration 3.

Physical models and experiments (Exp)

Several test campaigns have been carried out on centrifugal and non-centrifugal models (in England and France, and more recently in Asia), in purely cohesive, purely frictional, and then frictional cohesive and stratified soils. The failure of the working face is generally caused by the displacement of a rigid wall or the deflation of a flexible membrane at the working face (Figure 3a).

These models are valuable since on the one hand, they help to identify the kinematics of the fracture mechanism that should be considered in semi-empirical and analytical models (Limit Equilibrium (LE) and Yield Design (YD) described below), and on the other hand, they help to evaluate the face collapse pressures under controlled conditions, although they do not cover the whole range of variations of the different parameters.

Respecting similarities in conditions and minimizing scale effects makes experimental set-ups and the characterisation and installation

of materials somewhat complex. Validating calculation models can prove difficult, as data obtained from feedback on instabilities encountered in real full-scale structures is often incomplete and in particular data on deformation and failure mechanisms, as well as data on material properties. Some information from face instabilities observed *in situ* during excavation work using conventional methods and tunnel boring machines is given in the appendix.

Models based on the Limit Equilibrium approach (LE)

This approach is the one most commonly used in current practice: it consists of directly assessing the forces in play (Figure 3b). Its implementation in soil masses, or materials that can be considered as continuous at the scale of the structure, requires strong assumptions regarding:

- the geometry of the mechanism: the face being assumed rectangular, the most classical mechanism (Horn, 1961) is made up of a wedge, delimited by an inclined plane in front of the face and two triangular lateral faces, as well as a vertical right prism with a rectangular base rising to the surface (3D extension of the Terzaghi mechanism),

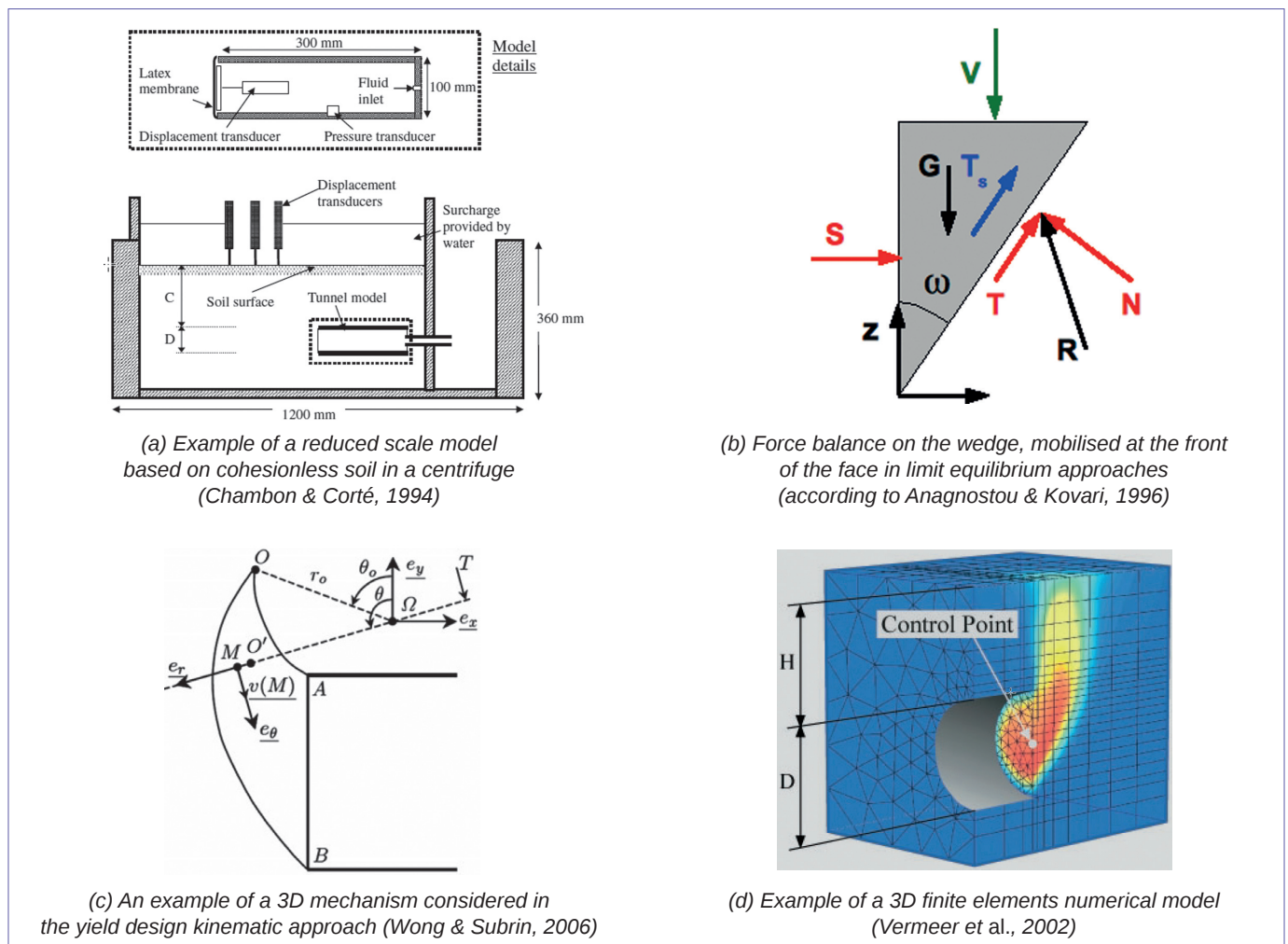


Figure 3: Examples of face stability models.

- the profile of the stresses (or their global resultant) applied on each face of the mechanism: the shear strength is defined by the Coulomb strength criterion (possibly Tresca) and the normal stresses on the fracture surfaces presuppose a value of the ratio between the horizontal and vertical stresses in the ground.

The principle consists in comparing the driving forces (weight of the wedge and vertical stress on its upper surface, possible surface overload, flow forces) with the mobilisable resistant forces (shear resistance of the ground on the different faces of the wedge and face pressure simulating the effect of a confinement).

It is possible to take into account horizontally stratified ground (e.g. in the context of a sedimentary basin) and to consider the effect of a water table without changing the failure mechanism considered.

Models developed within the framework of the Yield Design (YD) theory

Face stability conditions can be estimated by the yield design theory (Salençon, 1990), the results of which are similar to those of the limit analysis, if it is assumed that the associated ground has perfectly plastic rigid behaviour.

Based on the determination of statically admissible stress fields, the static approach, known as the interior approach, leads to a default estimate, therefore from a safety point of view, of the domain of bearable loads. In other words, if it is possible to find a stress field in the ground that verifies the equilibrium equations, the stress boundary conditions and the strength criterion, then the stability of the working face is assured. In the case of a collapse mechanism, as the face pressure is a loading parameter that opposes instability, this approach leads to an upper bound of the face collapse pressure.

In contrast, the kinematic approach, known as the external approach, is derived from the proposal of kinematically admissible virtual collapse mechanisms (Figure 3c), *i.e.* verifying the velocity boundary conditions. For a family of mechanisms characterised by a set of geometrical parameters, the power of the external forces is compared to the power of dissipation that the ground can mobilise given its resistance capacities. Optimisation with respect to the geometry of the mechanism leads to a lower bound of the face collapse mechanism: for the calculated value, face collapse is certain.

Compared to limit equilibrium approaches, the optimal geometry of the failure mechanism results from the calculation by optimisation of the geometric parameters of the considered mechanism family. The result does not depend on the initial conditions regarding the stress state. The models developed in homogeneous media are not directly applicable in the case of heterogeneous grounds since the stress and velocity fields require the verification of continuity conditions between materials of different characteristics.

This approach, although not widely used, has the merit of proposing possible value brackets and enabling collapse conditions to be determined by means of a rigorous approach, hence enabling the relevance of limit equilibrium approaches (based on more numerous assumptions) to be verified. The virtual failure mechanisms constructed “by hand” in the framework of the kinematic approach can be refined by numerical approaches.

Numerical models (Num)

The numerical models (Figure 3d) considered consist in solving the system with partial derivatives resulting from equilibrium equations, the ground's behaviour law, boundary conditions and initial conditions, by rewriting the problem in discrete form (in finite elements or explicit finite differences). The finer the mesh used, the more precise the solution. Given the three-dimensional nature of the mechanisms involved at the face, the calculation times required to obtain acceptable precision may be significant. Special attention should be paid to the representativeness of the assumptions made: radial blocking of nodes at the periphery of the face, vertical face pressure gradient (especially in the case of large diameter tunnels), mechanical characteristics of the ground, etc.

This type of deformation approach is used to estimate the collapse conditions, either by simulating the progressive reduction of the pressure at the face, or by using a method consisting in reducing the resistance parameters. Compared to the external approach of the Yield Design Theory, the search for the deformation and fracture kinematics is carried out among an “infinite” number of possible geometries, with optimisation resulting from the numerical calculation without fixing the fracture geometry *a priori*.

Starting from an initial state of geostatic stress in the ground, face collapse can be sought by progressively decreasing the face pressure, simulating the test procedure usually practised in laboratory experiments. The isovals of the plastic shear strains then allow the geometry of the fracture mechanism to be shown, and in particular the fracture surfaces to be highlighted in the case of rigid block mechanisms. The limit face pressure leading to collapse can also be estimated by representing the evolution of the extrusion of certain points of the face as a function of the reduction in face pressure.

If the face is self-stable (*i.e.* for zero face pressure), the associated safety margin can be estimated by gradually decreasing the shear strength of the ground until collapse (so-called “c-phi reduction” method), and adopting an approach where ground parameters are weighted.

ASSESSMENT OF STABILITY CONDITIONS

In this section and for each of the four calculation configurations (A, B, C, D) identified in §2.3, the different existing models are presented successively according to the four approaches (Exp, LE, YD, Num) explained in §2.5.

Many scientific articles have been devoted to the study of face stability over the last forty years. By way of illustration, it is worth mentioning that, at the time of writing, nearly 100 articles are referenced

under the keyword “*tunnel face stability*” in the international scientific journals “*Tunnelling and Underground Space Technology*” and “*Computers and Geotechnics*”, 60 of which were for the period 2018-2020 (3% of the articles published in these journals).

The references cited are not exhaustive and do not retrace the history of the work that led to the construction of all these models: all the “intermediate” models have not been mentioned.

3.1 DISCONTINUOUS MEDIUM

In moderately fractured rock masses, comparable to discontinuous mediums at the scale of the structure, face instabilities lead to dihedral falls or slides isolated by the network of discontinuities (Figure 4).

The geometry of the collapse mechanisms is dictated by the orientation and dip of the discontinuities with respect to the tunnel axis, their extension, their space and the shape of the face. The natural stability of these dihedra depends on the density of the rock and on the shear strength that can be mobilized on the discontinuities (function of the roughness of the wall rocks, their opening, possible filling, the presence of water, etc. The phenomenon of prevented dilatancy is an essential factor in the natural stability of underground excavations in rock).

As such, the design process can be summarised in the form of the following steps:

- **Identification of geometric and geomechanical data on discontinuities:**

The main families of discontinuities, their orientation and average spacing are assessed using the structural analysis of the massif deduced mainly from information from field surveys and core drilling.

The shear strength of discontinuities can be measured from shear tests on discontinuities in the laboratory, or from Barton's (1977) work on surface condition (JRC) and wall rock strength (JCS). In the absence of bolts or with unprestressed bolts, it is recommended by AFTES WG30 (2021) not to retain cohesion on the discontinuities (residual strength).

- **Identification of potentially unstable blocks:**

The geometry of the largest blocks that can slide at the face is assessed with a stereographic projection-based approach, or through 3D numerical modelling. A bolting set-up to ensure general stability can be deduced from this (see the following point). The stability of smaller sized blocks (local stability) can be provided thanks to the shear strength of sprayed concrete, or by releasing these small unstable blocks.



Figure 4: Example of instability in rock mass in the Chavannes tunnel (France).

- **Calculation of the safety factor for each block and calculation of the bolting scheme required to obtain an acceptable safety factor:**

The safety factor is calculated, in the limit equilibrium approach, by the ratio between the driving forces (weight of the block) and the strengths (shear strength along the discontinuities and the contribution of the bolting). The bolts have two effects: on the one hand, they directly take on part of the weight of the dihedron, and on the other they increase the shear strength that is available along the faces of the dihedron, by increasing the normal stress there if they are prestressed. These two effects are, of course, to be integrated into the stability calculations.

A safety factor of the order of 1.6 to 1.8 can be sought, by analogy with the values recommended in AFTES WG30 (2021) for radial bolting in the interior zone. For situations where the excavation is conducted for a long time, the required coefficient can increase up to 2.0.

3.2 CONTINUOUS UNDRAINED MEDIUM

When tunnelling at high speed in isotropic homogeneous low-permeability ground, it can be legitimately assumed that the ground behaves as undrained, whatever the boring method (conventional or TBM tunnelling), even if the necessary conditions (see §2.3) are rarely combined in practice. In this context, the ground strength criterion can be considered to be of the “Tresca” type (purely cohesive soils) characterised by the undrained shear strength (or in other words “undrained cohesion”) C_u . Figure 5 summarises the main references given over to this subject.

Broms & Bennermark (1967) are the first known authors to have taken an interest in this issue. They performed laboratory tests using a cylindrical sample of clay contained in a steel cylinder,

with a 2-cm diameter hole modelling the face. The assembly was placed on a triaxial test frame. First, a vertical stress σ_0 was imposed on the sample, and then the normal stress on the hole p_0 was gradually reduced until the face collapsed (Figure 6).

These analyses lead the authors to write the stability condition of the face, in purely cohesive ground, in the form of equation [5], where N is called the “stability number” and in fact expresses a load factor relative to the strength of the ground.

$$N = \frac{\sigma_s + \gamma \cdot H - \sigma_T}{C_u} \tag{5}$$

Case	Type	Reference	Brief description
Homogeneous continuous undrained medium	Exp	Broms & Bennermark (1967)	First laboratory tests carried out in Sweden with an experimental device similar to a triaxial cell with a hole allowing the extrusion of the soil ; Analysis of face instabilities on 14 excavation sites ; Introduction of the "stability number".
		Kimura & Mair (1981)	Centrifuge tests carried out in Cambridge, England, with a tunnel modelled as a 60 mm pressurised tube. Different lengths of unsupported span (zero to "infinite", <i>i.e.</i> plane deformations) and overburden thicknesses studied.
		Bezuijen & Van Seters (2006)	Centrifuge tests in Delft, the Netherlands, with a tunnel modelled as a 150 mm pressurised tube.
	LE	Perazelli & Anagnostou (2017)	Adaptation of the model of Anagnostou (2012) carried out in cohesive-frictional ground, to the purely cohesive case. The novelty lies in the calculation of the vertical force V acting on the dihedral, deduced from the static approaches of Gunn (1980), instead of a "Terzaghi" type discharge vault.
		Champagne de Labriolle (2018)	Extension of the model of Perazelli & Anagnostou (2017) by considering a circular geometry of the working face (instead of rectangular) and a more realistic distribution of horizontal stresses along the sliding surfaces.
	YD	Davis <i>et al.</i> (1980)	Kinematic approach: several cases studied including a 3D mechanism with two blocks (elliptical cylinders). Static approach: spherical and cylindrical stress fields, and comparison with experimental results in the case of a plane strain collapse mechanism in the cross section.
		Mollon <i>et al.</i> (2013)	Kinematic approach: 3D mechanism with a torus shape.
Num	Ukrichton <i>et al.</i> (2017)	3D finite element calculations taking into account a linear increase of C_u with depth.	

Figure 5: Summary of existing approaches in "undrained" conditions.

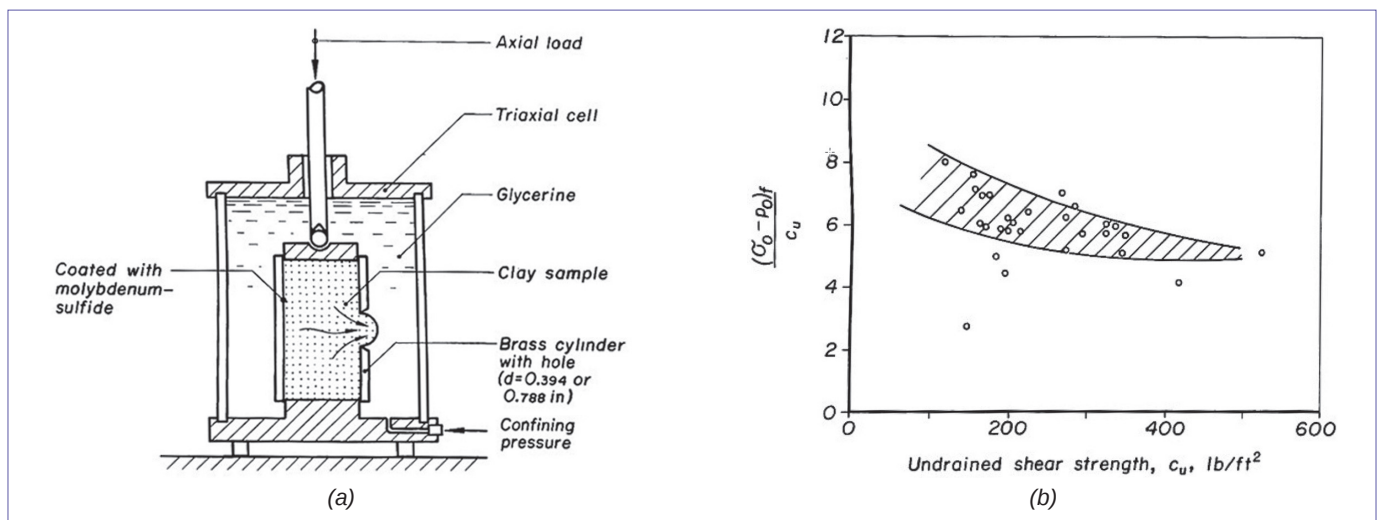


Figure 6: Broms & Bennermark Laboratory Tests (1967): (a) experimental device, (b) summary of results.

Broms & Bennermark (1967) also summarized the stability conditions observed at the face during eleven sewerage pipe jacking operations (diameters between approximately 0.8 and 2.3 m) carried out in Sweden, as well as three tunnels approximately 7 m in diameter in Norway and the United States, for overburden thicknesses of between 1.5D and 4D approximately. Most have stability numbers less than 6, without major face instabilities. The experience of the Tyholt Tunnel (Norway) in 1950 is interesting however, with two face instabilities, for C/D (overburden thickness/diameter) ratios equal to 2.0 and 2.2 respectively, and stability numbers of the order of 6.2 and 7.8. The length of the unsupported span during the collapses is not known. Compressed air pressure was then imposed in the tunnel, reducing the stability numbers by 2 units, thus ensuring stability.

Centrifugal tests on a scale model of a tunnel were then carried out in Cambridge on clays (Schofield, 1980; Kimura & Mair, 1981). The tunnel was modelled in the form of a pressurized half-tube 60 mm in diameter, increased to an acceleration of the order of 120g, i.e. modelling a real tunnel of around 7 m in diameter. Different overburden thicknesses ($1.2 < C/D < 3.3$) were studied, as well as different lengths of unsupported span d , between 0 (displacements allowed only at the face), and infinity (study in the interior zone of an unsupported tunnel).

These tests clearly demonstrate that:

- the collapse mechanism affects the entire face (Figure 7a),
- the lower sliding surface is inclined at less than 45° horizontally, which leads to a mechanism extending quite far in front of the face (almost a diameter at tunnel axis height),
- the initial mechanism spreads very rapidly to the surface when the overburden is shallow (1 to 2D) with a final sinkhole advancing to about 2D in front of the face, and 0.5D to the rear,
- there is no clear shear surface inside this mechanism.

The numerical models carried out later by Ukrichton et al. (2017) also confirmed these experimental observations (Figure 7b).

Bezuijen & Van Seters (2006) also conducted two centrifugal tests at Delft University for shallow overburden thicknesses (C/D equal to 0.6 and 0.8). The geometry of the collapse mechanism observed is not described by the authors, but the values of the stability numbers associated with the collapse are provided (see Figure 8).

Different theoretical approaches have been developed in parallel by different authors. In the field of yield design, mention may be made of the work of Davis et al. (1980) and Mollon et al. (2013), concerning the kinematic approach (approach from the outside). Davis et al. (1980) considered different mechanisms in the interior zone of the tunnel, but also a mechanism at the face (zero unsupported span), consisting of two elliptical cylinders. Mollon et al. (2013) improved it by considering a torus-shaped collapse mechanism. Regarding the static approach, Davis et al. (2013) studied different stress fields with cylindrical or spherical geometry at the face.

Among the limit equilibrium approaches, Perazzelli & Anagnostou (2017) extended the approach developed in the case of frictional cohesive ground (see §3.3) to the case of purely cohesive ground. The main modification made concerns the calculation of the vertical stress exerted on the upper face of the dihedron. Contrary to the cohesive-frictional case where it is deduced from a Terzaghi mechanism, based on the assumption of vertical sliding surfaces, here it is, deduced from the static approach to yield design in accordance with Gunn's work (1980). Three forms of stress fields in ground located above a rectangular trap are proposed by Gunn: a cylindrical geometry stress field the axis of which is parallel to the length of the trapdoor (i.e. longitudinally to the tunnel in our case), a stress field with a cylindrical geometry, the axis of which is parallel to the width of the trapdoor (i.e. transversely to the tunnel in our case), and a spherical geometry stress field encompassing the trapdoor. The minimum vertical stress value derived from these three forms is used.

Champagne de Labriolle (2018) improved the Perazzelli & Anagnostou (2017) approach by considering the cylindrical geometry of the tunnel. The integration of the stresses considers slices (of tiny heights) of variable width over the height of the face, contrary to the Perazzelli & Anagnostou (2017) approach in which the face is considered rectangular. Finally, Ukrichton et al. (2017) carried out numerical finite element calculations by considering a circular tunnel and a zero unsupported span. Perazzelli & Anagnostou (2017) also performed two numerical calculations in finite differences with a square tunnel cross-section.

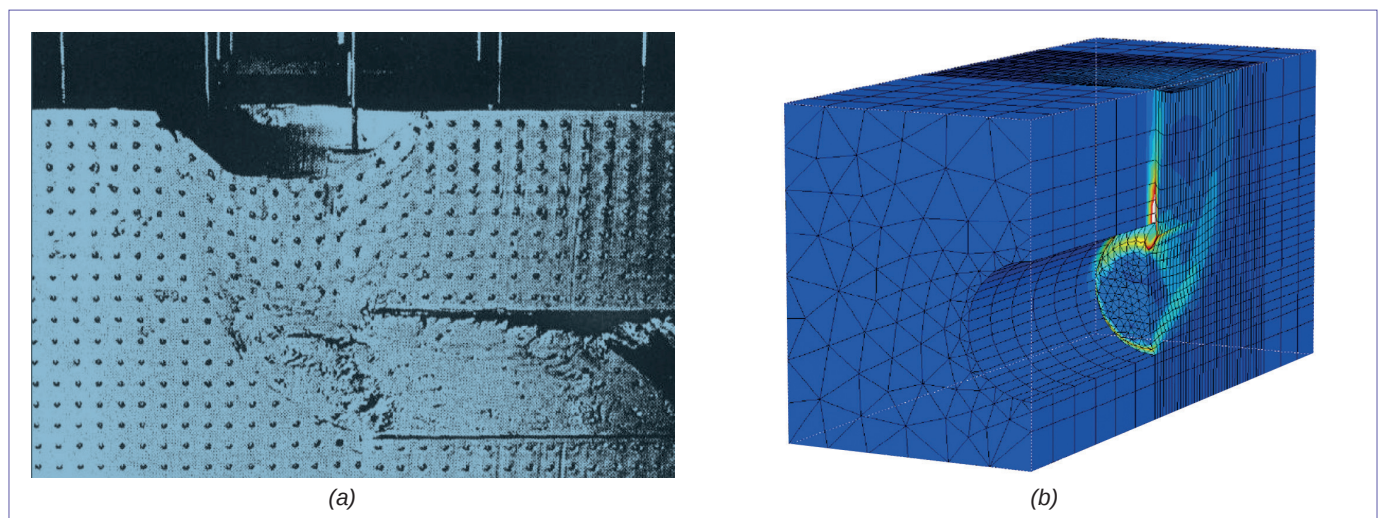


Figure 7: Mechanism geometry: (a) Centrifugal tests by Kimura & Mair (1981), (b) numerical modelling by Ukrichton et al. (2017).

Figure 8 compares the stability numbers N obtained by these different approaches in the case of a zero unsupported span and a constant "undrained cohesion". This summary firstly shows that the experimental results, notably Kimura & Mair (1981), are based on:

- approaches from the outside, for which the collapse is certain, whether they be of the "kinematic approach to yield design" type (Davis *et al.* (1980), improved by Mollon *et al.* (2013)), or of the numerical type (Ukrichon *et al.* (2017) and Perazzelli & Anagnostou (2017)). It should be noted that the difference between the two previous numerical approaches can be related to the geometry considered (square or circular face), but also to the rather coarse mesh considered by Perazzelli & Anagnostou (2017),
- approaches from the inside, for which the face is potentially stable, whether they are of the "static approach to yield design" type (Davis *et al.*, 1980) or "limit equilibrium of the dihedron taking into account a vertical stress on the dihedron deduced from the static approach to yield design" (Perazzelli & Anagnostou (2017), Champagne de Labriolle (2018)).

The disparity between these two broad categories of approaches remains quite large, around 30%. For example, for a tunnel 10 m in diameter, with a 15-m thick overburden, bored in a ground with 30 kPa of "undrained cohesion", the stability number is between 6.5 and 9, which leads to a limit pressure at the face, without safety factors, of between 130 and 200 kPa.

Note also the following limitations to the approaches mentioned above:

- static approaches to yield design consider simple stress fields, which it is difficult to imagine as being fully representative of the stress state around the face,
- the limit equilibrium models are based on a wedge, delimited at the level of the cutting face by a flat sliding surface, contrary to experimental observations which tend to consider a spiral arc,
- it is surprising that such a large gap exists between the numerical and experimental approaches.

In view of the previous developments, the face collapse limit pressure can thus be calculated from equation [7], integrating the principle in §2.4 that takes safety into account. The choice of the value of the critical stability number N_{crit} is to be made by the engineer on the basis of Figure 8, within the illustrated bracket. Lower values within the bracket lead to a safer design.

$$\sigma_{T-eff} = \sigma_s + \gamma \cdot H - N_{crit} \cdot \frac{C_u}{FS} + \Delta P_c, FS = 1,4,$$

N_{crit} chosen on Figure 8,

$$\Delta P_c = \begin{pmatrix} 10 \text{ kPa (SS)} \\ 30 \text{ kPa (EPB)} \\ 0 \text{ otherwise} \end{pmatrix}, \left[\begin{array}{l} \forall d/D \leq 0,2 \\ \forall C_u / (\gamma \cdot D) > 0,3 \end{array} \right]$$

[7]

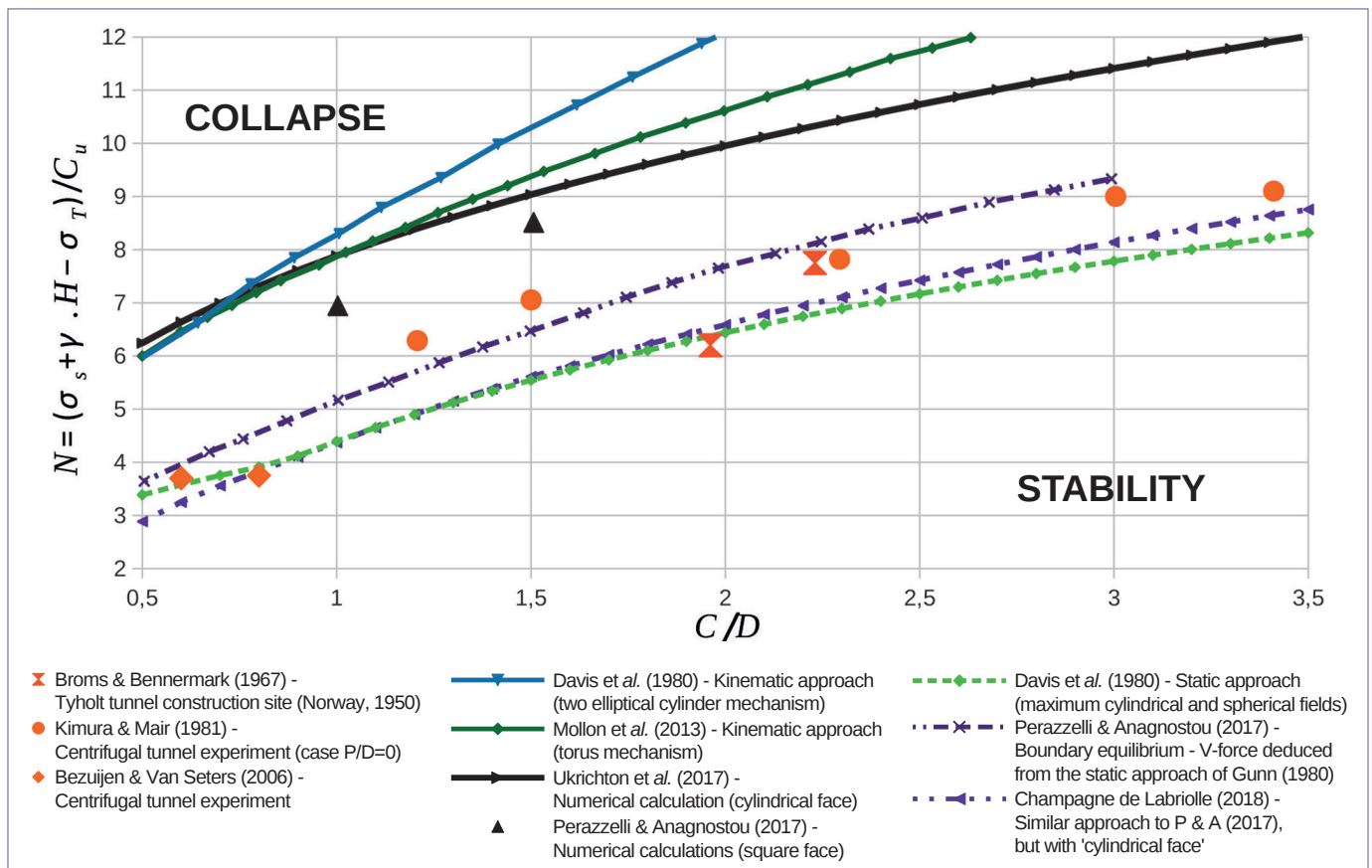


Figure 8: Comparison of the stability numbers deduced from the different existing models.

The influence of the length of the unsupported span on the stability of the face has also been studied by various authors. Mention may be made, in particular, of the Kimura & Mair centrifugal tests (1981), carried out for a large unsupported span, equal to 0.5D, 1D, 2D and infinite (*i.e.* equivalent to a stability calculation in the interior zone of the tunnel). The results obtained reveal significantly lower stability numbers in "plane strains" (infinite unsupported span) than in the case of a zero unsupported span (N divided by about two). For an unsupported span limited to 0.2D, it can be estimated that the stability number is reduced by about 0.5 according to the conclusions obtained by the authors.

The analytical calculations by Champagne de Labriolle (2018) result in the same order of magnitude for an unsupported

span 0.2.D long (see the author's Figure 24) in the case of an "undrained cohesion" greater than or equal to 50 kPa (*i.e.* $C_u / (\gamma \cdot D) > 0.3$).

For very low "undrained cohesions" ($C_u / (\gamma \cdot D) < 0.3$), the influence of the unsupported span in the Champagne de Labriolle (2018) approach is greater than indicated in the previous paragraph.

Some authors, notably Ukrichton *et al.* (2017) and Champagne de Labriolle (2018) have integrated a changing "undrained cohesion" depending on the depth. The results obtained are not presented here since it is rare, in practice, to have sufficient test results to demonstrate this change in shear strength depending on the depth.

3.3 CONTINUOUS DRAINED MEDIUM WITHOUT SEEPAGE

3.3.1 Homogeneous ground

In the case of permeable soil and a low advance rate (as an indication, as previously, for $k > 10^{-6}$ m/s and $v_{avct} < 0.1$ m/h), the ground is solicited in a "drained" state. The stability of the face is in this case conditioned by the effective stresses exerted in the ground. Let's consider that there is no seepage of pore water into the ground (water pressures remain equal to the initial hydrostatic pressures). This condition is encountered if the boring takes place outside the water table or if a pressurized TBM is used (except for the conditions described later in §3.5 and 3.6).

In this configuration, calculations are performed in effective stresses with:

- the density γ^* of the ground equal to: $\gamma^* = \gamma_{sat} - \gamma_w$ (soil unit weight under buoyancy) if the tunnel is below the water table, or γ_h (moist soil unit weight) if the tunnel is outside the water table,
- the drained shear strength, expressed as effective cohesion c' and an internal friction angle ϕ' in the context of a Mohr-Coulomb criterion.

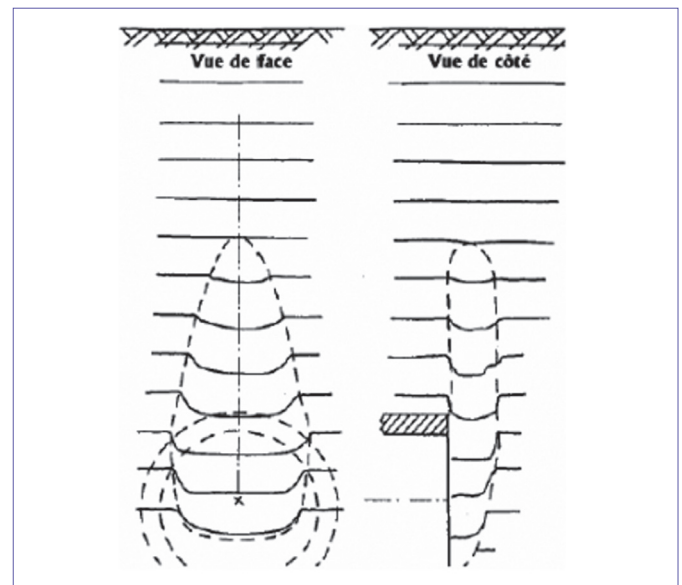


Figure 9a: Geometry of the collapse mechanism in cohesive-frictional ground (cross and longitudinal sections): Chambon & Corte (1989) tests.

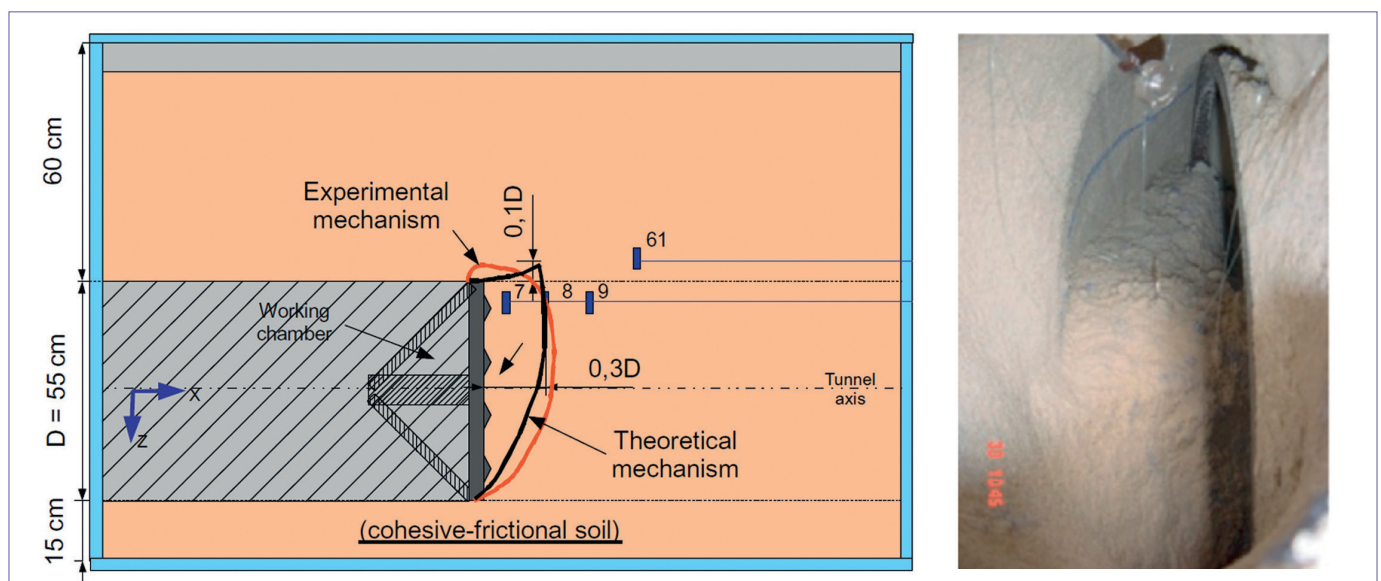


Figure 9b: Geometry of the collapse mechanism in cohesive-frictional ground (cross and longitudinal sections): Berthoz *et al.* (2012) tests.

The case of partially saturated soils is usually treated by considering an "apparent" effective cohesion and friction angle deduced from laboratory tests conducted on soil taken in a state of saturation identical to that observed on site.

Different testing campaigns were carried out in the laboratory in this configuration.

Examples include:

- Tests carried out by Chambon & Corté (1989) in a centrifuge with dry sands, where the boring is generated by deflating a flexible membrane at the face, with constant radial support by means of a metal tube,
- Tests performed by Berthoz *et al.* (2012) on a scale model of a non-centrifuged earth pressure TBM, with dry sands or slightly moist sands, giving them a cohesion of a few kPa, which corresponds to about ten kilopascals at full scale.

Case	Type	Reference	Brief description
Homogeneous continuous medium drained without seepage	Exp	Chambon & Corté (1989)	Centrifugal tests of rigid tubes with flexible faces on frictional cohesive ground → Shape of the mechanisms, and face pressure value for some H/D values.
		Messerli <i>et al.</i> (2010)	Non-centrifugal tests of rigid tubes with displaceable faces on dry sands → Shape of the mechanisms, and limit face pressure values for some H/D values.
		Berthoz <i>et al.</i> (2012)	Non-centrifugal model tests in purely frictional and cohesive frictional soils → Shape of the mechanisms, and limit face pressure values for some values of c' .
	Num	Vermeer <i>et al.</i> (2002)	3D finite element models with perfectly plastic elastic ground behaviour governed by a Mohr-Coulomb criterion, and displacement allowed only at the face (radial displacements blocked at the wall). Different values of dilatancy angle and earth pressure coefficient at rest were tested, with no significant effect on collapse pressure.
		Alagha & Chapman (2019)	A model similar to that of Vermeer <i>et al.</i> (2002) was used, with some additional parametric studies.
	LE	Anagnostou & Kovari (1996)	Horn (1961) type mechanism. Equilibrium of the wedge at the face with these assumptions: (1) rectangular front (B^*H), (2) vertical force on the wedge deduced from a relief arch with $\sigma_H = K_1 \sigma_{v0}$ where $K_1 = 0.8$, (3) shear force along the corner deduced by assuming that the vertical stress increases linearly with depth over the height of the prism, with the horizontal stress proportional via a factor $K_2 = 0.4$.
		Anagnostou (2012)	The model of Anagnostou & Kovari (1996) is modified by: (1) deleting the previous assumption (3) and replacing it with a "discharge arch" type analysis in the horizontal plane, (2) choosing $\sigma_H = 1.0 \sigma_v$ (instead of 0.8) for the block and the prism (assumption (2)).
		DAUB (2016)	Recommends using the method of Anagnostou & Kovari (1996) but with a coefficient $K_2 = (K_0 + K_a)/2$ instead of 0.4.
		Champagne de Labriolle (2018)	Modifications to the model of Anagnostou & Kovari (1996) by: (i) expressing K from the assumption that the criterion is verified on the boundaries of the mechanism (thus relationship between σ_v and σ_H , which are not necessarily principal constraints); (ii) considering the circular character of the working face (instead of rectangular).
	YD	Leca & Dormieux (1990)	Kinematic approach: initial model: one or two 2D blocks.
		Wong & Subrin (2006)	Kinematic approach: 3D one-block model defined by logarithmic spirals without internal discontinuity surface.
		Mollon <i>et al.</i> (2011)	Kinematic approach: 3D model with a large (but variable) number of discontinuity surfaces cutting blocks defined by logarithmic spiral arcs.
		Zou <i>et al.</i> (2019)	Kinematic approach: modifications to the model of Mollon <i>et al.</i> (2011) by replacing the part of the mechanism located above the tunnel crown by a pressure deduced from a "limit equilibrium" type mechanism with an assumption of normal stress on this mechanism (K_s) drawn from various approaches (analytical, numerical, experimental).
		Li <i>et al.</i> (2019)	Kinematic approach: using the geometry of the Wong & Subrin (2006) model, considering a partially saturated soil.
		Quarmout <i>et al.</i> (2019)	Kinematic approach: 3D model with two blocks (a tetrahedron at the face, and a prism with a triangular base above). Resolution by the KEM method (Kinematic Element Method), which is not exactly Yield Design, but is similar.
		Li & Yang (2020)	Kinematic approach: 3D one-block mechanism defined by logarithmic spirals with no internal discontinuity surface, and with truncation of the tensile strength criteria.
Senent <i>et al.</i> (2020)		Kinematic approach: 2D 3-block mechanism, considering the existence of a unsupported span. Possible consideration of an umbrella arch.	

Figure 10: Summary of existing approaches in continuous homogeneous medium drained without seepage.

These tests, the results of which are shown in Figure 9, reveal that the mechanism:

- affects the entire face,
- is not very far from the front of the face (less than 0.5 D) and rises slightly above the crown (approximately 0.1 D for an internal friction angle of around 35°),
- can propagate to the surface by progressive collapse in the case of low overburden.

Many numerical and analytical models have also been devoted to this configuration. Figure 10 gives the main references.

The numerical modelling carried out by Vermeer et al. (2002) or Berthoz et al. (2012), confirm these main features of the mechanisms observed in a frictional-cohesive medium, on which various recent analytical models have been based (Wong & Subrin (2006), Mollon et al. (2011), etc.).

The minimum face collapse pressure associated with this type of mechanism can be expressed as the following equation:

$$\sigma_{T-eff} = \max(\sigma'_{T-eff}; 0) + FSE \cdot \gamma_w \cdot H_w$$

$$\text{with } \sigma'_{T-eff} = N_y \cdot \gamma^* \cdot D - \frac{c'}{\tan(\varphi')}$$

$$[9] \quad \gamma^* = \begin{pmatrix} \gamma_{sat} - \gamma_w \text{ (under the water table)} \\ \gamma_h \text{ (outside the water table)} \end{pmatrix}, \Delta P_c = \begin{pmatrix} 10 \text{ kPa (SS)} \\ 30 \text{ kPa (EPB)} \\ 0 \text{ otherwise} \end{pmatrix}$$

Different authors expressed the N_y function in equation [9] via different approaches. Figure 11 summarises the results.

Ultimately, all the approaches cited here converge. Vermeer et al. (2002) also performed numerical calculations considering a non-zero unsupported length d . They have shown that N_y increases quite significantly (i.e. the minimum necessary pressure to exert on the face and in the unsupported span increases), when the unsupported length becomes greater than about 0.3 D. Senent et al. (2020) also showed this via an analytical approach to yield design (2D longitudinal mechanism with 3 blocks defined by logarithmic spirals).

Given the consistency between these different results, the expression [10], deduced from Vermeer et al. (2002) can be used for most of the cases encountered in practice ($d/D \leq 0.5$, $C/D \geq 0.8$ and $\varphi' \geq 20^\circ$).

$$\sigma_{T-eff} = \max(\sigma'_{T-eff}; 0) + FSE \cdot \gamma_w \cdot H_w$$

$$\text{with } \sigma'_{T-eff} = N_y \cdot \gamma^* \cdot D - \frac{c'}{\tan(\varphi')} + \Delta P_c$$

$$\text{where: } N_y = \frac{2+3 \cdot (d/D)^{6 \cdot \frac{\tan \varphi'}{FS}}}{18 \cdot \frac{\tan \varphi'}{FS}} - 0,05 \quad \begin{cases} \forall d/D \leq 0,5 \\ \forall \varphi' \geq 20^\circ \\ \forall C/D \geq 0,8 \end{cases}$$

$$FS = 1,25, FSE = 1,05,$$

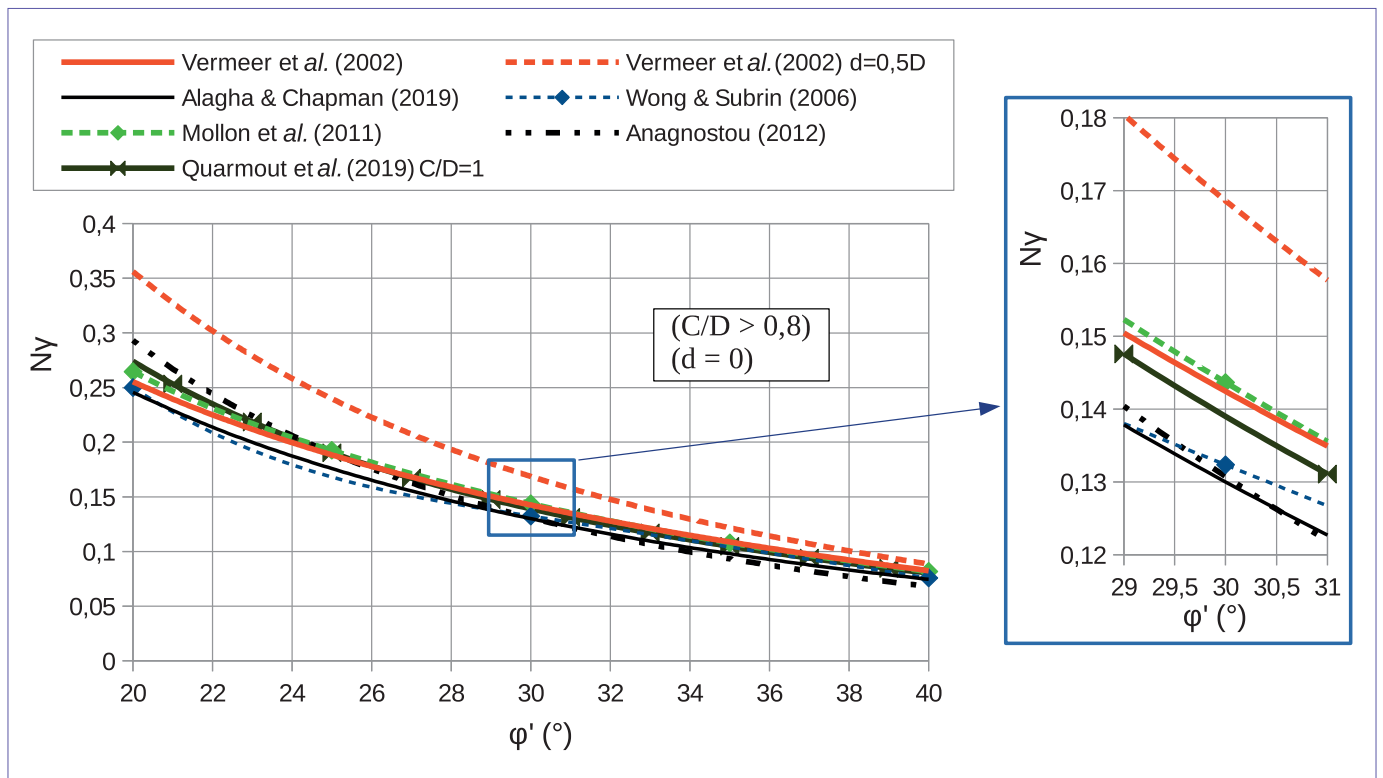


Figure 11: Comparison between different existing models.

In the context of the kinematic approach for yield design, the mechanism can intercept the surface of the natural ground in the case of a very shallow tunnel in low friction ground (typically for approximately $C/D \leq 0.3$ ($\cot \varphi' - 1$)). The minimum face stability pressure is then a function of the surface overload σ_s and can be expressed in the form of an equation [11] (Wong & Subrin 2006), analogous to the classical yield design approaches for shallow or deep foundations.

$$\sigma_{T-eff} = N_y \cdot \gamma \cdot D - N_s \cdot \sigma_s - (1 - N_s) \cdot \frac{c'}{\tan(\varphi')} + \Delta P_c \quad [11]$$

Numerical calculations by Alagha & Chapman (2019) also show that the influence of the overburden thickness (C/D ratio) becomes significant when the internal friction angle of the soil is very small ($\varphi' < 20^\circ$). This hypothesis of a very shallow tunnel and very low friction ground is however rare among projects.

All the numerical and analytical models presented consider a Mohr-Coulomb strength criterion with a non-zero tensile strength of the soil. Li & Yang (2020) performed analytical calculations (with the kinematic approach to yield design) and numerical calculations with this hypothesis to evaluate the influence of this questionable hypothesis in soils. The calculations performed show that conventional approaches (without truncation of the tensile criterion) tend to underestimate the confinement pressures at collapse. This underestimation remains low for $\varphi' \geq 20^\circ$ and $c' \leq 20$ kPa (Figure 12) but becomes significant in the case of low friction and highly cohesive ground ($\varphi' \leq 20^\circ$ and $c' \geq 20$ kPa). In practice, however, soils having such shear strengths may probably be considered as "undrained" and thus treated by the approach described in §3.2.

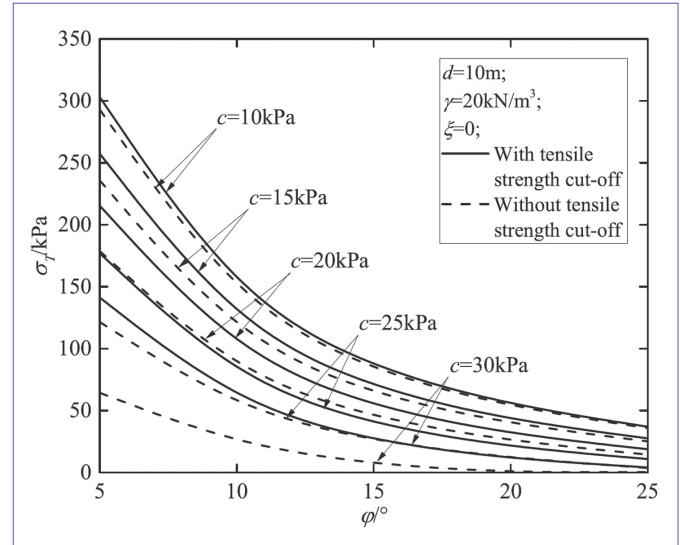


Figure 12: Influence of tensile strength on face collapse limit pressures (Li & Yang, 2020). Here, d is the tunnel diameter (D) and $\xi = 0$ means that the criterion is not truncated at all.

In purely frictional ground (dry or saturated sands), a seepage mechanism originating at the crown and rising to the surface, like an "hourglass" (Figure 13), can be mobilized according to the scale model tests carried out by Berthoz et al. (2012). In practice, this type of solid grain seepage mechanism could only be encountered in the case of tunnelling with an earth pressure TBM outside the water table in sands. Indeed, in conventional tunnelling methods, field treatment would be required, and bentonite would be injected into the slurry pressure TBM. The latter two cases would lead to the existence of cohesion over a short length of ground at the front of the face, preventing the appearance of this seepage mechanism. In all of these cases, using the equation [10] approach with zero cohesion is safe.

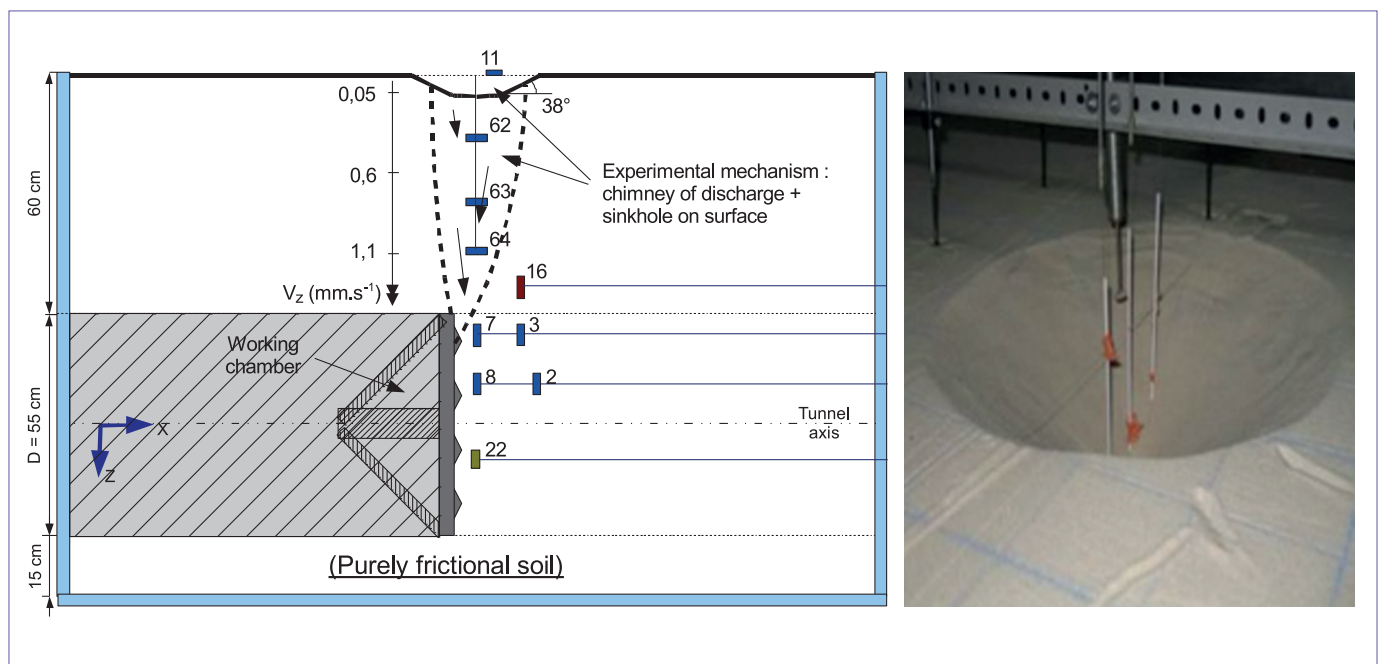


Figure 13: Geometry of the collapse mechanism in purely frictional ground (Berthoz et al., 2012).

3.3.2 Layered grounds

Some authors have extended the previous approaches to the case of horizontally stratified grounds, with layers of different shear strengths, but always with the assumption that they are individually isotropic. Figure 14 provides a brief overview of these.

In particular, we should note the physical models in stratified ground produced by Berthoz et al. (2012). These tests have highlighted the associated collapse mechanisms, as shown in Figure 15 in the case of a three-layer ground (lower part of the face self-stable frictional cohesive, upper part of the face purely frictional, with a frictional cohesive overburden).

Berthoz (2012) also extended the Wong & Subrin (2006) mechanism to the case of a two-layer stratified mass where the

upper part of the face (height $\beta.D$) has a shear strength lower than that of the lower part. The decrease in the associated factor N_y (i.e. the increase in stability caused by the reduced dimensions of the face) is given in Figure 16b.

Limit Equilibrium (LE) approaches make it quite easy to take into account several layers of different shear strengths, over the height of the face and in the thickness of the overburden, such as the developments presented in Broere (2001), adopted by Vu et al. (2015) and Champagne de Labriolle (2018). These two models consider a "wedge and vertical prism" type mechanism similar to that of Horn (1961), adopted by Anagnostou & Kovari (1996), but with some specificities, such as the consideration of the arching effects, via the K ratio between vertical stress and horizontal stress.

Case	Type	Reference	Brief description
Seepage-free drained stratified continuous medium	Exp	Berthoz et al. (2012)	Non-centrifugal tests with a reduced scale model in two-layered and three layered grounds → Shape of the mechanisms.
	LE	Piakowski & Kowalewski (1965)	The face is divided into ten "slices", heightwise. For each slice, the pressure at the face is calculated as a function of the active ground pressure (Rankine theory) and a shape coefficient allowing for arch effects.
		Broere (2001) and Vu et al. (2015)	The approach is identical to that of Anagnostou & Kovari (1996) but with: (1) the face split into slices, allowing application, (2) horizontal arching effects taken into account via the choice of $K_1 = K_2 = K_0$ and replacing R by $R/(1+\tan\theta)$.
		Champagne de Labriolle (2018)	Homogeneous soil approach transposable by reasoning by horizontal layers of different shear strength.
	YD	Berthoz (2012)	Extension of the model of Wong & Subrin (2006) to the case of a stratified bilayer medium.
		Ibrahim et al. (2015)	Extension of the model of Mollon et al. (2011) to the case of a stratified bilayer medium.
		Pan & Dias (2017)	Extension of the model of Mollon et al. (2011) to the case of a non-circular tunnel. Finally, the case studied is similar to that studied by Berthoz (2012) and Ibrahim et al. (2015).
		Zou et al. (2019)	Extension of the model of Mollon et al. (2011) to the case of a linear evolution with depth of the ground cohesion and friction angle.

Figure 14: Summary of existing approaches in a seepage-free stratified drained continuous medium.

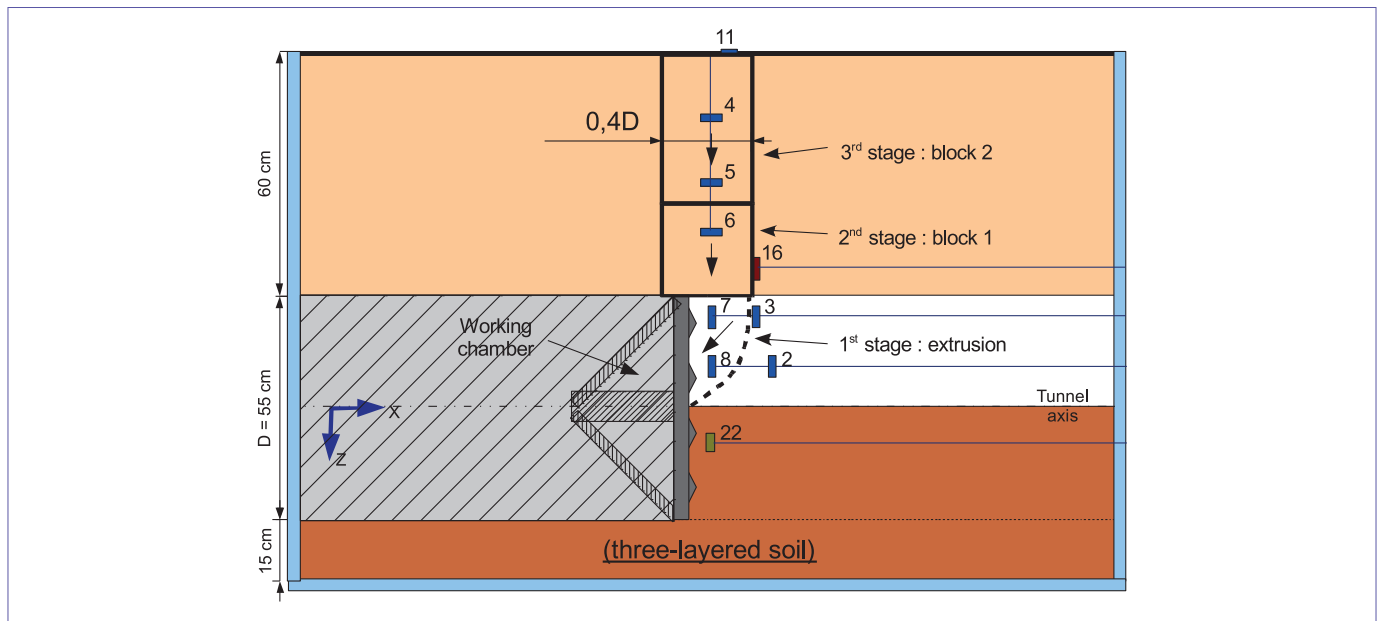


Figure 15: Collapse mechanism in stratified ground (purely frictional layer between two cohesive frictional layers) (Berthoz et al., 2012).

However, his work remains rather difficult to use since there is no direct expression of the result: a spreadsheet is required. When working on a project, if the strength contrasts between the different layers are not too significant, then an initial approach can be to consider the shear strength of a homogeneous medium as equal to that of the weakest actual layer. In the case

of a strong contrast, with one very strong layer in the upper part (rocky slab), the mechanism can simply be truncated at the lower (soft) part of the face, the vertical stress exerted on the wedge being automatically reduced due to the cohesion considered in the upper layer. If the very strong layer is in the lower part of the face, a reduced face height can simply be considered.

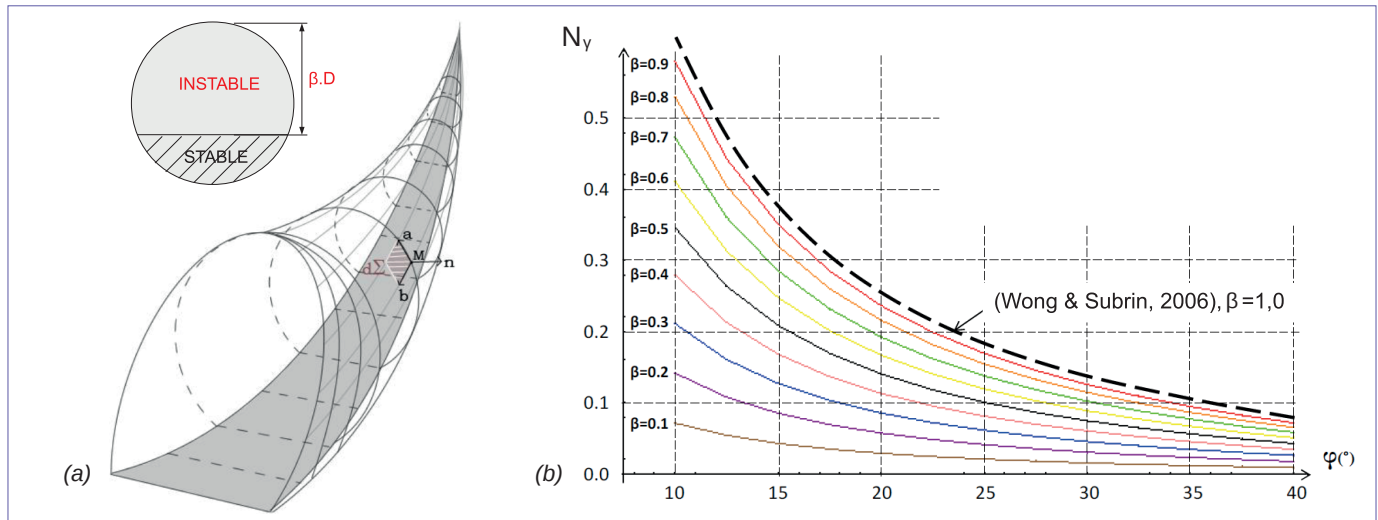


Figure 16: Two-layer stratified ground (Berthoz, 2012): (a) Mechanism geometry, (b) nomograph.

3.4 CONTINUOUS DRAINED MEDIUM WITH SEEPAGE

3.4.1 Seepage towards the face

When boring a tunnel by the conventional method or with an open-face TBM in water-saturated ground, seepage towards the face appears with seepage forces decreasing the stability of the face. The main authors who have studied this problem are indicated in Figure 17.

The seepage force reaches its maximum when the hydraulic steady state is reached with a maximum flow rate. Most calculations carried out in this case are done so in a conservative manner and consider that the steady state has been reached.

This hypothesis is legitimate to the extent that the permeability of the ground k is greater than or equal to 10^{-7} to 10^{-6} m/s and that the face advance rate v_{avct} is less than or equal to 0.1 to 1 m/h (as an indication according to Anagnostou & Kovari (1996)). It should be remembered that the assumption of an isotropic ground is made, both in terms of shear strength and permeability. Schuerch et al. (2019) have, however, also studied the transient phase of the seepage, quantifying the length of time during which the face remains stable in the short term. This question is posed, for example, during hyperbaric maintenance operations on the cutterhead of pressurized TBMs.

Case	Type	Reference	Brief description
Continuous drained medium with seepage towards the face	Exp	Lü et al. (2018)	Non-centrifugal tests on a reduced-scale model in dry, saturated no-flow, and saturated flowing sands. Comparison of mechanisms and limit collapse pressures.
	Num	Schuerch et al. (2019)	3D finite element modelling with hydro-mechanical coupling for transient analysis.
	LE	Perazelli et al. (2014)	Extension of the model of Anagnostou (2012) by taking into account the flow forces towards the tunnel. For this purpose, the hydraulic load h is assumed to depend only on the distance to the face x for the wedge, with an expression calculated through numerical finite element modelling of the flow.
	YD	Pan & Dias (2016)	Extension of the model of Mollon et al. (2011) by adding a component N_w modelling the flow forces ($i \cdot y_w$) to the classical effective stress calculation (function of N_v). N_w is deduced from a flow calculation on Flac.
		Pan & Dias (2018)	Extension of the Pan & Dias (2016) model to the case of a Hoek & Brown plasticity criterion taken into account via an optimization of the mechanism geometry as a function of the internal friction angle corresponding to the linearization of H&B and keeping a couple (c, φ) consistent with the initial H&B criterion (if φ increases, c decreases and N_c increases).

Figure 17: Summary of approaches for a continuous drained medium with seepage towards the face.

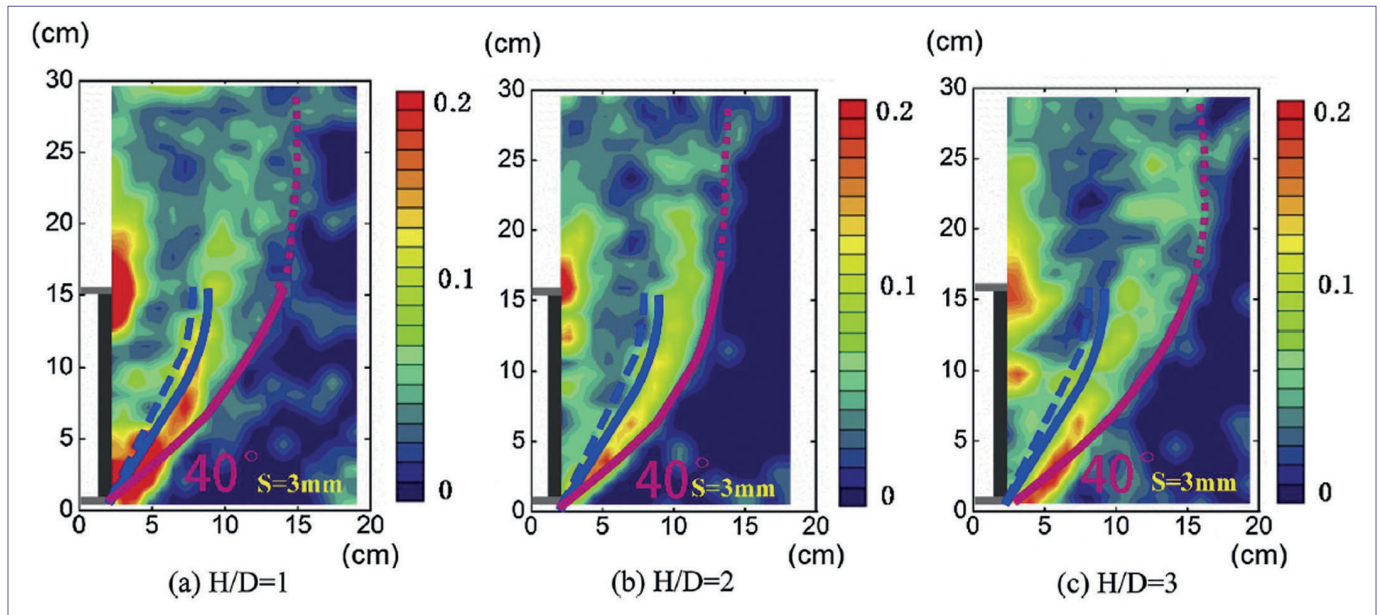


Figure 18: Results of experiments by Lü et al. (2018): geometry of the mechanisms in the presence of a seepage (purple) for different water table heights (H) relative to the tunnel crown. The mechanisms observed for dry (dotted blue line) and saturated grounds without seepage (solid blue line) are also presented for comparison. The axes of the x and y coordinates correspond to the distances with respect to the foot of the face. The colour scale corresponds to the plastic strain isovalues.

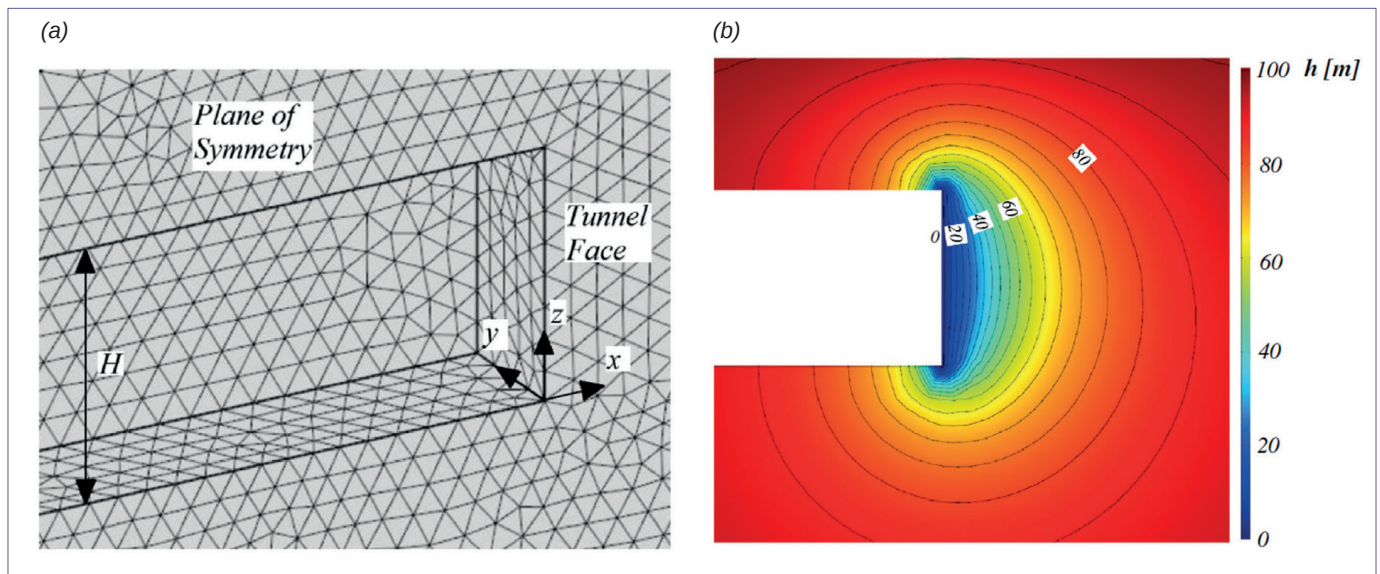


Figure 19: Finite element calculations of seepage forces from Perazzelli et al. (2014): (a) mesh, (b) hydraulic load isovals.

Let us first consider the steady state reached. Lü et al. (2018) conducted tests on an uncentrifuged model, with a tunnel of $D = 15$ cm in diameter and an overburden thickness between 0.5 and 2.D. The ground is made up of sands. Given the d_{10} of this sand (about 85 microns), its permeability is around $5 \cdot 10^{-5}$ to 10^{-4} m/s according to the Hazen relationship (AFTES WG8, 2006). The instability of the face is generated by pushing back a rigid plate. Three test conditions are studied: dry sand, sand saturated with water but without seepage ("watertight" plate at the face) and water-saturated sand with seepage (totally permeable plate at the face).

These tests show that the seepage forces lead to a lower inclination of the mechanism sliding surface in the presence of seepage (about 40° relative to the horizontal according to

Figure 18) than the same dry (63°) or saturated material (57°) without seepage. The mechanism consequently extends further out in front of the face in the presence of seepage forces, and mobilises a larger volume of earth at collapse.

Different analytical models have been developed to evaluate the face pressure σ'_T required in the presence of seepage. In these models, the seepage forces are estimated using numerical calculations (with finite elements or finite differences) as shown in Figure 19. These are then injected into the face stability analytical models presented in the preceding paragraphs. Perazzelli et al. (2014) adapted Anagnostou & Kovari's limit equilibrium model (1996) and Pan & Dias (2016, 2018) extended the yield design model of Mollon et al. (2011).

The calculations performed by the various authors show that:

- the instability of the face increases significantly when the water height increases (see Figure 20), which is explained by the increase in the amplitude of the (driving) seepage forces when the hydraulic gradient increases,
- the instability of the face increases when the density of the ground decreases (dotted lines compared to the solid lines in Figure 21b),
- the trends are similar, but there is a disparity between the results obtained by Perazzelli et al. (2014) and Pan & Dias (2016, 2018). This difference depends in particular on the amplitude of the hydraulic load (Figure 20),
- horizontal permeability of the ground greater than the vertical permeability (anisotropy) improves the stability of the face compared to the isotropic case of minimum permeability (Pan & Dias, 2016).

Analyses in transient conditions by Schuerch et al. (2019) on the basis of the coupled hydro-mechanical finite element calculations, made it possible to assess the duration during which the seepage forces remain sufficiently low for the front to remain stable. Different values for the hydraulic load, overburden thickness and earth pressure at rest coefficients were studied. Nomographs were deduced from it. For example, Figure 21 shows the maximum duration of self-stability (left) and the confinement pressure required in steady

state (right) in a particular case. These figures are deduced from Schuerch et al. (2019) and Perazzelli et al. (2014), after standardising the notations used. The red dots correspond to the following assumptions with the notations in Figure 2: $D = 10$ m, $H_w = H = 15$ m, $\gamma = 20$ kN/m³, $K_0 = 1$, $k = 10^{-8}$ m/s, $E = 20$ MPa, $c' = 25$ kPa and $\phi' = 25^\circ$. With these assumptions, these calculations show that the critical duration t_s of auto-stability of the face is equal to 700 s, and that a pressure σ_T equal to 15 kPa must be applied to the face in steady state to ensure its stability.

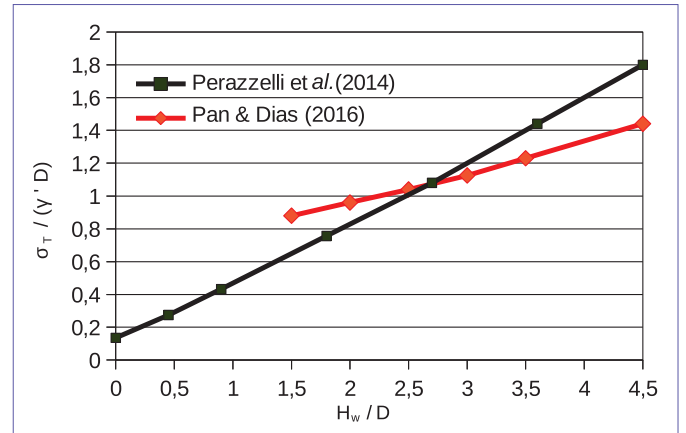


Figure 20: Comparison of existing solutions with the following assumptions: circular tunnel of diameter D , $\gamma_w / \gamma' = 1.0$ (i.e. $\gamma = 20,0$ kN/m³), $c' = 0$ kPa, $\phi' = 30^\circ$.

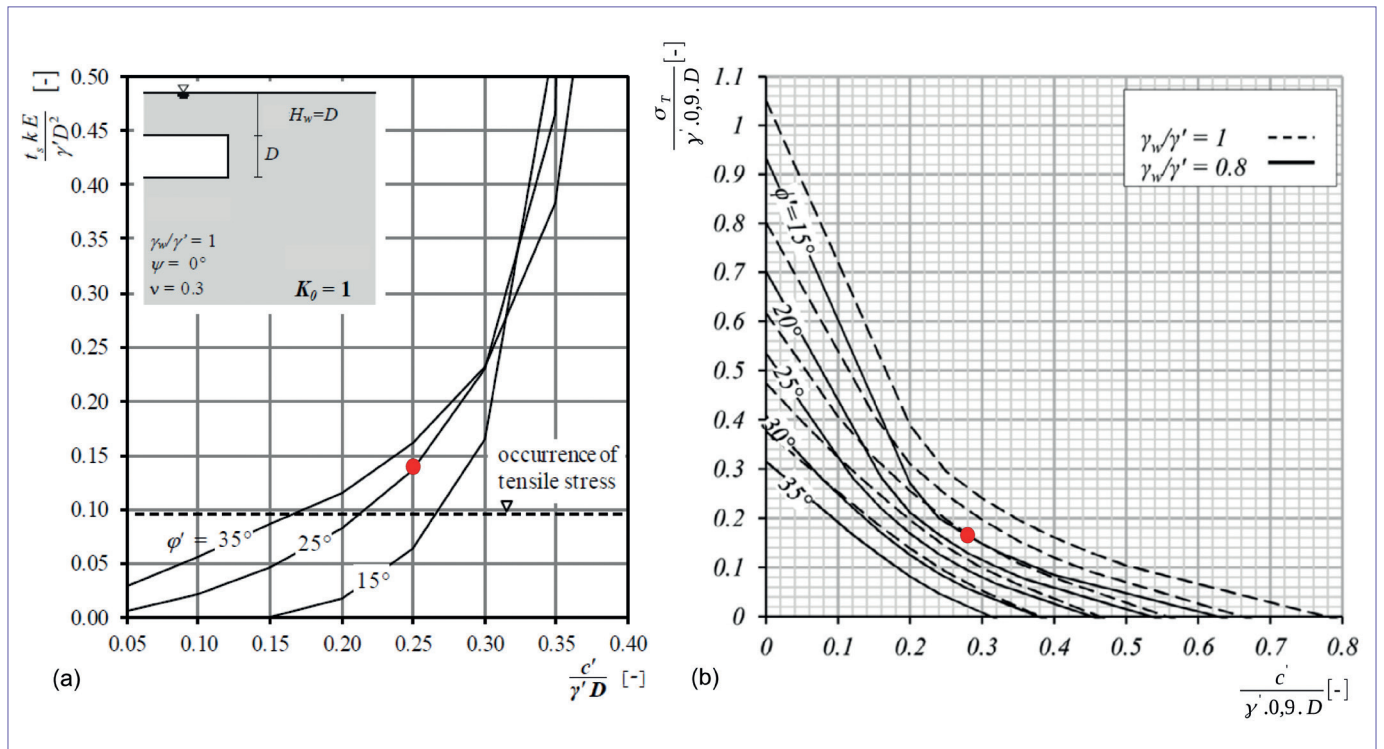


Figure 21: (a) Assessment of the stability limit duration, according to Schuerch et al. (2019), and (b) assessment of the containment pressure necessary to ensure steady-state stability, according to Perazzelli et al. (2014). In these two figures, the notations have been modified to be consistent with those in Figure 2. They correspond to the following case: $H_w = H = 1.5 D$, $K_0 = 1$. The two red dots correspond to the case described in the body of the text.

3.4.2 Seepage towards the ground

Boring with a pressurized face TBM can generate pore overpressures in the ground in front of the face, thereby reducing the effective stresses, including the shear strength on the collapse surfaces of the face instability mechanism.

Measurements made by Xu & Bezuijen (2018) in the Netherlands during boring with a slurry pressure TBM in sands ($10^{-5} < k < 10^{-3}$ m/s) show that these reach 50 kPa in the immediate vicinity of the face and 10 kPa 10 m in front of the face (Figure 22a). During the segment laying phases (boring is stopped), these overpressures dissipate quickly until they cancel each other out (return to hydrostatic pressure). This phenomenon has also been measured by the same authors in the case of earth pressure tunnelling using admixtures (Figure 22b), with overpressure peaks which are even greater in the case presented (100 kPa in the immediate vicinity of the face, and 20 to 30 kPa 10 m ahead of the face). The associated boring conditions are not, however, described precisely by the authors.

Broere (2001) conducted analytical developments to express the amplitude of pore overpressures Δu as a function of the particle size (d_{10}) and of the permeability (k) of the ground, the shear strength of the bentonite (τ_c), and the initial hydrostatic pressure (u_0). The field of effective stresses at any point in the collapse mechanism can be deduced from this and applied to the models described in §3.4.

However, the parametric studies carried out by Broere (2001) show that taking into account pore overpressures when studying face stability leads to a small increase in face pressure (less than 20 kPa) in the vast majority of the cases studied.

Consequently, a first approach in this case (boring with a slurry pressure TBM or an earth pressure TBM with many fine admixtures in sandy soils with a permeability of between 10^{-5} and 10^{-3} m/s) could be to calculate the minimum face collapse pressure without taking pore overpressures into account, and then increase this pressure by a lump-sum of 30 kPa.

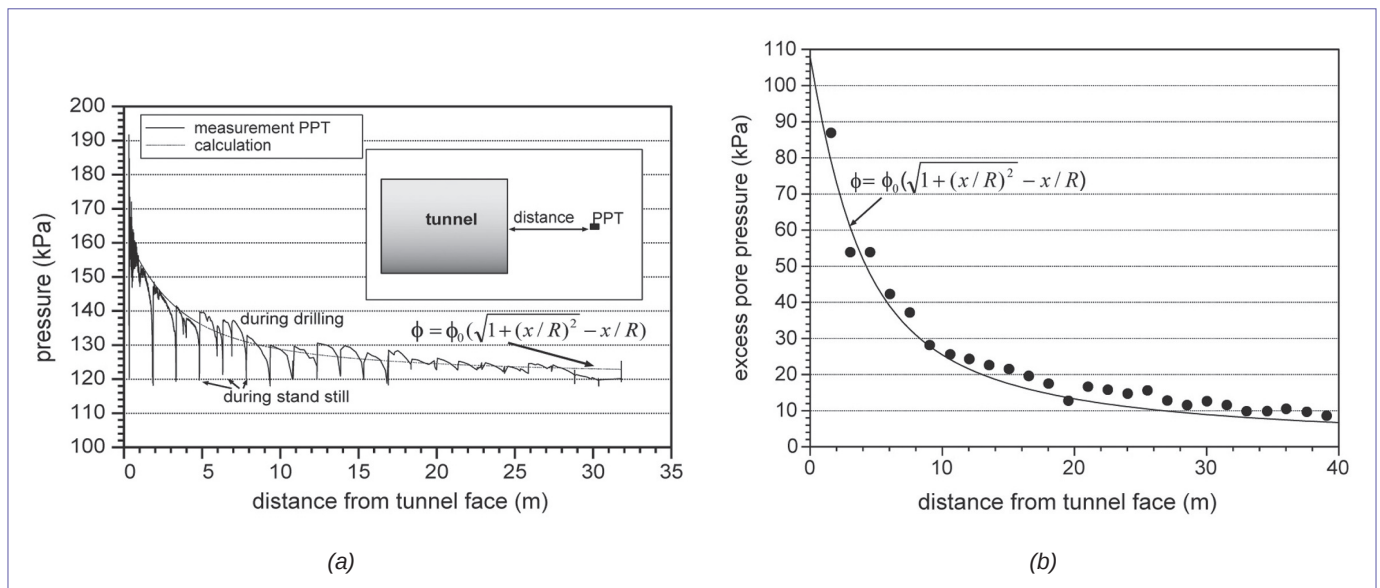


Figure 22: Pore overpressures measured in front of a slurry pressure TBM (a) and earth pressure TBM (b) by Xu & Bezuijen (2018).

ON-SITE OBSERVATIONS AND CONSTRUCTION MEASURES

This section deals with construction principles that ensure face stability, with recommendations in terms of face stability monitoring. Two cases must be distinguished: (i) the case of

conventional tunnelling, and (ii) the case of pressurized face TBMs. The case of open tunnelling machines is partly covered by the information given for conventional method tunnelling.

4.1 CONSTRUCTION METHODS IN CONVENTIONAL TUNNELLING

In conventional tunnelling, different processes may be applied to control face stability, notably cross-section reduction, drainage, face bolting and ground treatment. The following paragraphs outline some main principles for each of these process.

Cross-section reduction

The lower the height of the face, the greater its stability. Boring sections separately, (top heading, then bench), or maintaining a central merlon in place can therefore increase its stability. However, this is not without consequences on the use of wall supports and more generally the tunnelling advance rate.

Sprayed concrete layer

Although in practice calculations do not justify it, purging must be carried out, followed by the application of a thin layer of fibre-reinforced sprayed concrete on the face after each excavation sequence (3-5 cm thick), primarily to ensure the safety of workers and protect them from small block falls.

Indeed the effectiveness of the sprayed concrete comes from two actions. On the one hand, it protects the ground against surface alteration (by limiting desiccation caused by exposure of the ground to air and limiting water flow that may lead to out-wash and seepage forces). On the other, this layer of sprayed concrete has a very local mechanical action (of a centimetre magnitude), but sufficient to prevent micro-displacements, and consequently micro-ruptures, which would be likely to lead to a degradation of the characteristics of the mass in depth, by a phenomenon of "chain discohension: the grain of sand that escapes releases the stone that wedged the block, and so on" ("type 1" sprayed concrete within the meaning of AFTES WG20, 2001).

Drainage and dewatering

The calculations presented in section 3.4 have demonstrated, if necessary, the very negative impact of water on the stability of the working face. Pre-draining the water table or draining the ground as the face advances is therefore an excellent method of reducing pore pressures at the front of the face and preventing the development of significant seepage forces that are detrimental to stability. This drainage should preferably be peripheral in order to avoid local instabilities at the centre of the advancing tunnel face.

Zingg & Anagnostou (2016) performed analytical and numerical calculations of the stability of the face in soils ($0 < c' < 400$ kPa and $\phi' = 30^\circ$) by varying the number, length and position of these boreholes. The authors conclude, on the basis of charts quantifying the effect of drainage on the stability of the face, that a very good efficiency is obtained with 4 to 6 boreholes of 10 cm diameter and 1.5 D in length located near the tunnel wall, in the upper part of the face.

However, implementing dewatering and drainage as the tunnel face advances can lead to consolidation settlements over an extended area around the structure.

Face bolting

When the previous processes are insufficient, face bolting can be used.

In the case of discontinuous mediums, where the mechanisms are of the "dihedral fall" type, a few continuously anchored bolts of moderate length (up to 6 m) oriented according to the discontinuities are generally sufficient. The design of bolts is based on limit equilibrium methods in accordance with §3.1.

In the case of continuous or continuous equivalent mediums, long horizontal fibreglass bolts (generally 1.5 to 2.0 D, never less than 0.5 D) are required. The bolts must be long enough and changed regularly (generally by thirds) to ensure the stability and control of face strains at all times. In particular, the calculation should be made considering the shortest length of the bolts, *i.e.* just before their renewal.

There are several different approaches that can be used to calculate the length, cross-section and number of these face bolts. The simplest method consists in calculating the stress σ_T required to ensure the stability of the face using the approaches described in §2.5 and then, from this, deducing the total confinement force to be supported by the bolting. The number and cross-section of the bolts required to support this force without breaking the bolts, depends on the minimum anchoring length required given the lateral friction (q_s) that can be mobilised around each bolt, taking into account the fact that the anchoring must be verified over the "active" length (at the head) and over the "passive" length (at the foot) without reaching the tensile failure of the bolts (Peila, 1994). The AFTES WG30 recommendation (2021) provides further information on this point, notably with regard to the safety factors to be used and the determination of the value of the q_s .

Other more elaborate approaches that explicitly take into account bolts in the study of face stability are possible. An (old) summary of different design approaches is available in Clouterre (2002). These include the works by Leca (1997) and Subrin (2002) as part of the kinematic approach to yield design, or those more recent works by Anagnostou & Perazzelli (2015) using limit equilibrium. Nowadays, it is also possible to carry out 3D digital modelling with explicit bolt simulation (Zapata Franco (2020) for example), which also makes it possible to evaluate the effect of bolting on the displacements induced in the ground.

Umbrella vault

The main objective of an umbrella vault is to stabilise the unsupported span, and limit pre-convergence and convergence, *i.e.* limit displacements generated on the surface. However, an umbrella vault also has a beneficial effect on the stability of the face insofar as it reduces the volume of the collapse mechanism by truncating the upper part of it.

Different approaches to the designing of vaults are possible, ranging from simply calculating the hyperstatic reactions of an isolated tube subjected to a ground load estimated using a Terzaghi type mechanism, to 3D digital modelling. Some references can be found in Gilleron (2016) for example.

However, the effect of the umbrella vault on the stability of the face is limited. As an example, the 2D numerical and analytical calculations (yield design) carried out by Senent *et al.* (2020) in cohesive frictional grounds without seepage estimate that the presence of the umbrella vault reduces the confinement pressure required to ensure face stability by about 15%.

It should also be reminded here that installing an umbrella vault is a major construction process. Given the large diameter of the boreholes to be made, it is essential that the tubes be sealed one after the other, after the drilling of each hole, in order to avoid a "pre-splitting" of the ground and the appearance of very large settlements on the surface related to the installation phase prior to the actual excavation.

Ground treatments

Various ground treatment methods can be used with the purpose of increasing the overall shear strength of the ground and reducing its permeability. These include injections, freezing or jet-grouting.

The assessment of the mechanical characteristics of the soils treated is not of immediate interest. A sufficient safety margin must be considered during design, and control tests following treatments in test bore holes are recommended. At the design stage, readers interested may, for example, consult the following references to obtain initial information:

- for injections: cohesions between a few tens and hundreds of kilopascals are observed (Dano, 2001; Chang *et al.*, 2009; etc). The efficiency of large-scale treatment remains a difficult subject. The engineer must remain cautious about the cohesion value used in the design,
- for jet-grouting: orders of magnitude of the cohesions and permeabilities attainable are given by Croce *et al.* (2014) and Toraldo *et al.* (2018). The latter also offer a methodology for estimating the shear strength of grounds on a large-scale from uniaxial compression and sonic tomography,
- for freezing: ISGF WG2 (1992) proposes a first estimate of the mechanical characteristics of frozen soils, in particular the increase in their cohesion when the soil temperature decreases.

4.2 MONITORING METHODS IN CONVENTIONAL TUNNELLING

In conventional tunnelling, the face is visible after each excavation sequence. This time must therefore be used to validate the geotechnical assumptions (in the broad sense) made during the studies, and in particular to validate the stability conditions of the face. Face surveys are the formal manifestation of these. Examples of face surveys are available in Appendices 1 and 2 of AFTES WG24 (2008).

Regarding the "Validation of geotechnical hypotheses"

Important information includes:

- the nature of the ground,
- an order of magnitude of the shear strength of the ground derived from empirical observations (peelable with a knife, difficult to break with a hammer, etc.), pocket penetrometer tests in soils, or even Franklin tests for rock blocks,
- the orientation and condition of discontinuities in the rock masses,
- the number and flow rate of water inflows.

Parameters characterizing the fractured rock environment, based on Bienawski's Rock Mass Rating (1989), Barton's Q index (NGI, 2013) or Geological Strength Index (Marinos *et al.*, 2005) can also be deduced from the observations and compared to the expected values.

Regarding "Validation of face stability conditions"

Any signs of face instability are to be recorded during face surveys. These signs consist of falling blocks, the appearance of cracks in the face, extrusion movements (measured with an extrusometer, or topographic targets in the event of prolonged stoppage).

These clues must enable the support manager to determine if the face is self-stable or not, and if there is instability to identify the geometry of the mechanisms at play and the best way to adapt face support.

It is also important to ensure the bolts are correctly distributed at the face (make sure that their deviation remains moderate) and that they are properly sealed into the ground.

4.3 CONSTRUCTION METHODS FOR PRESSURIZED FACE TUNNELLING

Pressurized face tunnelling ensures face stability and limits the movement of the ground around the excavation. Different containment modes exist, depending on the nature of the material contained in the working chamber:

- **pasty containment**, where the working chamber is mainly filled with excavated materials, with some additives (water / foams / polymers / clay). These additives aim to make the confinement material sufficiently impermeable to limit internal water circulation, but not too viscous so that the torque on the cutter head remains reasonable, nor too liquid so that the muck can be transported easily by conveyor belt. This confinement mode is that exerted by earth pressure TBMs with a full working chamber,
- **liquid containment**, where the working chamber is filled with slurry. This slurry must be viscous enough to enable a water-tight membrane (cake) to be created at the face enabling pressure to be effectively exerted on the granular skeleton of the ground. However, it must not be too viscous so that excavated material can be easily transported to the slurry treatment plant, and be easily recycled.

This confinement mode is that exerted by slurry pressure TBMs,

- **gas containment**, where the working chamber is filled with compressed air. This confinement mode is that used by air pressure TBMs, but also by earth pressure TBMs when the working chamber is partially filled, or by earth pressure and slurry pressure TBMs during hyperbaric operations.

In all cases, these systems require the identification of a "set value" face confinement pressure to ensure the stability of the face, to contain hydrostatic pressures and, where relevant, to limit admissible movements in the presence of neighbouring structures.

The issue of containment pressure along the shield is also paramount: if this is very low, the stability of the face will be degraded (adopt the approach for boring with a non-zero unsupported span in the theoretical approaches previously described). More broadly, experience shows that the pressure prevailing along the shield directly conditions the amplitude of the displacements induced on the surface in the case of shallow tunnelling.

The “closed” mode of pressurized face TBMs does not provide accurate information about the nature of the ground or the actual stability conditions of the face. The lower bound of the stability domain is therefore unlikely to be re-assessed during the work. Nevertheless, hyperbaric interventions can be used to make a partial survey of the face.

However, the area of “admissible displacements” and the resulting set value pressure are to be adjusted regularly during the work using the retro-analysis of the displacements measured as part of the Tunnelling Advance Plan (TAP), made by successive tunnel boring sections. This tool, which is intended to be dynamic and iterative, has the following goals for the contracting authority, the project manager and the contractor:

- summarise in one single and shared document, and by project section, the expected geological, hydrogeological and geotechnical conditions, the set values of the key parameters of the machine, the necessary controls, the spatial identification of possible residual risks, etc.,
- summarise the feedback as the tunnelling advances and reuse it for successive tunnelling sections within the same project, and also for future projects,
- improve the boring rate, for example through the possibility of integrating feedback to review the confinement pressures,

- better control impacts on neighbouring structures, when necessary.

To meet these goals, the tunnelling advance plan (TAP) (AFTES WG16, 2020) must be accompanied by:

- a summary of the data collected during the work: (i) the probing data of neighbouring structures and the ground, (ii) the geotechnical model data, and (iii) the tunnelling steering conditions data (pressures in the working chamber, thrust force on the cutter head, total thrust force, fontimeter measurements, extracted masses, etc.),
- comparison of these “real” data with the assumptions used in the studies,
- retro-analysis is used to recalibrate certain model assumptions and enable the projected displacements induced to be updated for the remainder of the project (*i.e.* improved reliability of the reference scenario).

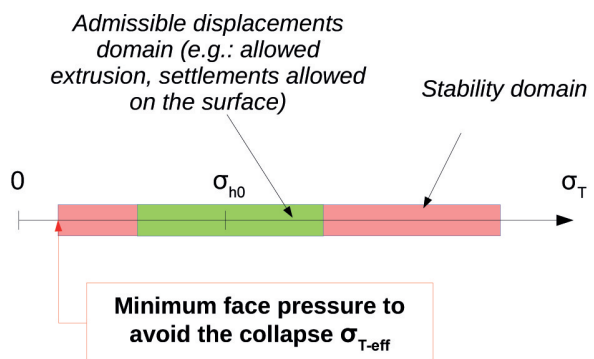
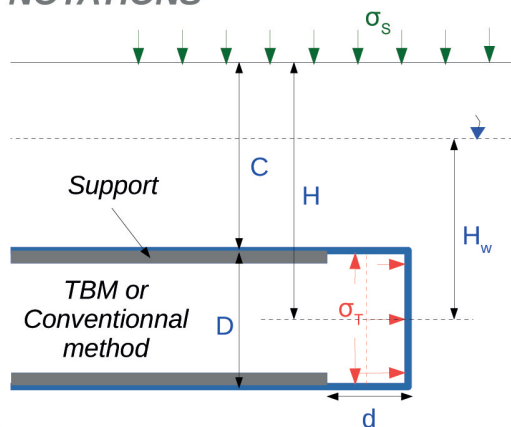
In order to address the above points and be useful during the work, the approach implemented must be sufficiently flexible and summarised in relatively simple formats (*e.g.* overview diagram on the longitudinal profile of the tunnel), be rapid and facilitate communication.

SUMMARY

WHY ENSURE FACE STABILITY?

- Guarantee the safety of workers,
- Limit impacts on neighbouring constructions in the case of shallow tunnels,
- Control the costs and time required to complete the work,
- Contribute to the sustainability of the structure by limiting overbreaks and decompressed areas.

NOTATIONS



CONTINUOUS DRAINED MEDIUM WITHOUT SEEPAGE

Scope: conventional tunnelling or open shield tunnelling without significant pore pressures in the vicinity of the face (naturally, or due to drainage), or pressurized face tunnelling.

Collapse mechanism: a block affecting the entire face, barely extended to the front (less than $0.5 \cdot D$), barely rising above the crown initially, but capable of propagating vertically by progressive collapse.

Calculation Method:

$$\sigma_{T-eff} = \max(\sigma'_{T-eff}; 0) + FSE \cdot \gamma_w \cdot H_w \quad \text{with} \quad \sigma'_{T-eff} = N_y \cdot \gamma^* \cdot D - \frac{c'}{\tan(\varphi')} + \Delta P_c$$

$$\text{where: } N_y = \frac{2 + 3 \cdot (d/D)^{6 \cdot \frac{\tan \varphi'}{FS}}}{18 \cdot \frac{\tan \varphi'}{FS}} - 0,05 \quad \left[\begin{array}{l} \forall d/D \leq 0,5 \\ \forall \varphi' \geq 20^\circ \\ \forall C/D \geq 0,8 \end{array} \right], \quad FS = 1,25, \quad FSE = 1,05$$

$$\gamma^* = \begin{pmatrix} \gamma_{sat} - \gamma_w & \text{(below the water table)} \\ \gamma_h & \text{(outside the water table)} \end{pmatrix}, \quad \Delta P_c = \begin{pmatrix} 10 \text{ kPa (SS)} \\ 30 \text{ kPa (EPB)} \\ 0 & \text{otherwise} \end{pmatrix}$$

Areas of vigilance:

- The above expression assumes an isotropic homogeneous ground. In the case of a face with mixed ground, several solutions are possible. If the strength contrasts remain low, consider the minimum strength of the different facies. If the contrasts are high, limit the geometry of the mechanism to low-strength layers (modification of D in the above equation),
- With an earth pressure TBM outside the water table without additives in clean sands, a different mechanism, of the "hourglass" type may appear. The use of the above equation is nevertheless safe.

CONTINUOUS MEDIUM WITH SEEPAGE TOWARDS THE TUNNEL

Scope: boring by the conventional method or with open shield tunnelling under the water table, hyperbaric operations on pressurized TBMs.

Calculation mechanisms and methods: the seepage forces further destabilise the face.

Two studies may be required:

- > To assess whether the face is stable under steady state conditions, the reader may refer to the nomographs in Perazzelli et al. (2014),
- > To assess the duration during which the seepage forces remain sufficiently low for the face to remain stable in transient conditions, refer to the nomographs in Schuerch et al. (2019).

CONTINUOUS UNDRAINED MEDIUM

Scope: high-speed boring in low-permeable ground ($k < 10^{-7}$ m/s and $v_{avct} > 0.1$ m/h).

Collapse mechanism: a block affecting the entire face, extending approximately 1.D to the front.

Calculation Method: $\sigma_{T-eff} = \sigma_s + \gamma \cdot H - N_{crit} \cdot \frac{C_u}{FS} + \Delta P_c$, $FS = 1,4$,

$$N_{crit} \text{ chosen on Figure 8, } \Delta P_c = \begin{pmatrix} 10 \text{ kPa (SS)} \\ 30 \text{ kPa (EPB)} \\ 0 \text{ otherwise} \end{pmatrix}, \left[\begin{array}{l} \forall d/D \leq 0,2 \\ \forall C_u / (\gamma \cdot D) > 0,3 \end{array} \right]$$

Areas of vigilance: pay attention to the stoppage periods on the construction site that could make the “undrained” assumption unrealistic.

DISCONTINUOUS MEDIUM

Scope and mechanisms: moderately fractured rock masses inducing dihedral fall mechanisms.

Calculation Method: (i) identification of geometric and geomechanical data for discontinuities, (ii) identification of potentially unstable blocks by stereographic projection or 3D modelling, (iii) calculation of the safety factor of each block (target: 1.6 to 1.8).

Areas of vigilance: pay attention to the orientation of families of discontinuities (and their persistence) and disregard the cohesion of discontinuities.

CONSTRUCTION METHODS IN CONVENTIONAL TUNNELLING

Different technical solutions are possible: Cross-section reduction (move to working with divided sections in particular), sprayed concrete (the effect of this thin layer remains localized but essential), drainage, face bolting, ground treatments, and possibly umbrella vault.

Monitoring during works: importance of face surveys to validate geotechnical assumptions, detect signs of instabilities, and ensure correct implementation of the above processes.

CONSTRUCTION METHODS WITH A PRESSURIZED FACE TBM

TBMs designed for face stability: three confinement modes are possible (pasty/ liquid / gaseous), the choice of which must be made depending on the geotechnical context of each project.

Monitoring during works: Importance of a tunnelling advance plan (TAP) summarising: (i) the data collected during the work (survey of the ground and neighbouring structures, mechanical characteristics of the ground, conditions for steering the TBM), (ii) the comparison between the actual conditions and the expected conditions, (iii) retro-analyses improving the reliability of the reference scenario.

GLOSSARY

Geometric parameters

D (m)	Tunnel diameter
C (m)	Overburden thickness
H (m)	Depth of the tunnel axis
d (m)	Length of the unsupported span

Geological, hydrogeological and geotechnical parameters

H_w (m)	Height of water in relation to the axis of the tunnel
k (m/s)	Ground permeability coefficient
γ (kN/m³)	Moist soil unit weight
γ' (kN/m³)	Soil unit weight under buoyancy
C_u (kPa)	"Undrained" cohesion of the soil
c' (kPa)	Effective cohesion of the ground
φ' (°)	Internal friction angle of the ground

Parameters related to boring and neighbouring structures

EPBS	Earth pressure balanced shield
SS	Slurry shield
σ_s (kPa)	Surface pressure
σ_T (kPa)	Pressure exerted on the face (assumed constant)
σ_{T-eff} (kPa)	Face pressure value to be exerted to prevent its collapse
V_{avct} (m/h)	Advance speed of the face

REFERENCES

- AFNOR (2005), *Eurocode 7 : Calcul géotechnique – Partie 1 : règles générales*. NF EN 1997-1, 138 p.
- AFTES WG8 (2006), *La conception et la réalisation des travaux d'injection des sols et des roches*, Recommandation R2F1, Tunnels et Espace Souterrain, n°194-195, pp. 70-154.
- AFTES WG16 (2020), *Effects caused by excavation on neighbouring structures in the design and construction of underground works*, Recommandation R2A1, 68 p.
- AFTES WG20 (2001), *Design of sprayed concrete for underground support*, Recommandation R1A1, Tunnels et Ouvrages Souterrains, n°164, pp.68-108.
- AFTES WG24 (2008), *Les reconnaissances à l'avancement*, Recommandation R1F1, Tunnels et Espace Souterrain, n°209, pp. 302-325.
- AFTES WG29 (2007), *Compatibilité des recommandations AFTES relatives aux revêtements des tunnels en béton avec les Eurocodes*, Recommandation R2F1, Tunnels et Ouvrages souterrains, n°204, 18 p.
- AFTES WG30 (2021), *Radial rock bolting in tunnels – Design and sizing guide*, Recommandation R1A1, 97 p.
- Alagha S.N, Chapman D.N. (2019), *Numerical modelling of tunnel face stability in homogeneous and layered soft ground*, Tunnelling and Underground Space Technology, vol. 94, pp. 1-14.
- Anagnostou G. (2012), *The contribution of horizontal arching to tunnel face stability*, Geotechnik, vol 35, n°1, pp34-44.
- Anagnostou G., Kovari K. (1996), *Face stability conditions with Earth Pressure Balanced Shield*, Tunnelling and Underground Space Technology, vol 11, n°2, pp. 165-173.
- Anagnostou G., Perazzelli P. (2015), *Analysis method and design charts for bolt reinforcement of the tunnel face in cohesive-frictional soils*, Tunnelling and Underground Space Technology, vol 47, pp. 162-181.
- Berthoz N. (2012), *Modélisation physique et théorique du creusement pressurisé des tunnels en terrains meubles homogènes et stratifiés*, Thèse de doctorat de l'ENTPE, 292 p.
- Berthoz N., Branque D., Subrin D., Wong H., Humbert E. (2012), *Face failure in homogeneous and stratified soft ground: Theoretical and experimental approaches on 1g EPBS reduced scale model*, Tunnelling and Underground Space Technology, vol. 30, pp. 25-37.
- Bezuijen, A., & van Seters, A. (2006). *The stability of a tunnel face in soft clay*. In H. van Lottum, & A. Bezuijen (Eds.), *Tunnelling; a decade of progress* (pp. 149-155). Taylor & Francis.
- Bienawski Z.T. (1989). *Engineering Rock Mass Classification*, Wiley, New York, 251 p.
- Broere W. (2001), *Tunnel face stability & new CPT application*, PhD Thesis, Delft university of technology, Delft university press.
- Broms B.B., Bennermark H. (1967), *Stability of clay at vertical openings*, Journal of Soil Mechanics and Foundations Division, vol. 93, pp. 71-94.
- CEDD (2015), *Catalogue of notable tunnel failures – case histories (up to April 2015)*, Civil Engineering and Development Department, Government of Hong Kong, <https://www.cedd.gov.hk>
- Chambon P. & Corté J.F. (1989). *Stabilité du front de taille d'un tunnel faiblement enterré: modélisation en centrifugeuse*, Proceedings of the Int. Conf. Tunnelling and Microtunnelling in Soft Ground: from field to theory, Paris, presses ENPC, pp. 307-315.
- Chambon, P., Corte, J.F. (1994). *Shallow tunnels in cohesionless soil: stability of tunnel face*, Journal of Geotechnical Engineering 120 (7), pp. 1148–1165.
- Champagne de Labriolle G. (2018), *Détermination de la fenêtre de pilotage de la pression de confinement d'un tunnelier fermé dans un sol cohérent-frottant ou purement cohérent*, Revue Française de Géotechnique, vol. 155, n°3.
- Chang M., Chen C.C., Huang R.C., Chang J., Yang P.J. (2009), *Investigation on mechanism of grouting and engineering characteristics of in-situ grouted soils*, Proceedings of the 17th International Conference on Soil Mechanics and Geotechnical Engineering, M. Hamza et al. (Eds.), pp. 2346-2349,
- Clouterre (2002), *Additif 2002 aux recommandations Clouterre 1991, pour la conception, le calcul, l'exécution et le contrôle des soutènements réalisés par clouage des sols*, Presses de l'École Nationale des Ponts et Chaussées, 217 p.
- Croce P., Flora A., Modoni G. (2014), *Jet-grouting technology, design and control*, London, UK : CRC Press (Taylor & Francis Group).
- Dano C. (2001), *Comportement mécanique des sols injectés*, Thèse de doctorat de l'Université de Nantes, 216 p.
- DAUB (2016), *Recommendations for Face Support Pressure Calculations for Shield Tunnelling in Soft Ground*, German Tunnelling Committee, 64 p.

- Davis E.H., Gunn M.J., Mair R.J., Seneviratne H.N. (1980). *The stability of shallow tunnels and underground openings in cohesive material*, Géotechnique, n°40, pp. 397-416.
- Gilleron N. (2016), *Méthode de prévision des tassements provoqués par le creusement des tunnels urbains et influence des présoutènements*, thèse de doctorat de l'université Paris-Est, 238 p.
- Grasso P., Xu S., Del Fedele M., Russo G., Chirioti E. (2003). *Particular failure mechanisms of weathered granite observed during construction of metro tunnels by TBM*, ITA World Congress, Amsterdam.
- Gunn M.J. (1980), *Limit analysis of undrained stability problems using a very small computer*, Proc., Symp. on Computer Applications to Geotechnical Problems in Highway Engineering, Cambridge Univ., Cambridge, UK, pp. 5–30.
- Horn, M. (1961), *Alagutak homlokbiztosítstasra ható vizszintes földnyomasgalat néhány eredménye*, Azorszdgos mélyépítőipari konferencia előadásai, Közlekedési Dokumentációs Vállalat, Budapest (in Hungarian).
- Ibrahim E., Soubra A.H., Mollon G., Raphael W., Dias D., Reda A. (2015), *Three-dimensional face stability analysis of pressurized tunnels driven in a multilayered purely frictional medium*, Tunnelling and Underground Space Technology, vol. 49, pp. 18-34.
- ISGF WG 2 (1992), *Frozen ground structures – Basic principles of design*, by Andersland O., Berggren A.L and Fish A., Ground Freezing 91, vol 2. pp. 503-513.
- Kimura, T. and Mair, R. J., (1981), *Centrifugal testing of model tunnels in soft clay*, Proceedings of 10th International Conference on Soil Mechanics and Foundation Engineering, Stockholm 1981, Vol. 1, pp 319-322.
- Leca E. (1997), *Développement d'outils de calcul pour le dimensionnement des tunnels creusés en terrains meubles*, Thèse d'habilitation, Université de Lille, 83 p.
- Leca E., Dormieux L. (1990), *Upper and lower bound solutions for the face stability of shallow circular tunnels in frictional material*, Géotechnique, vol. 40, n°4, pp. 581-606.
- Li T.Z., Yang X.L. (2020), *Stability of plane strain tunnel headings in soils with tensile strength cut-off*, Tunnelling and Underground Space Technology, vol. 95, pp. 1-11.
- Li Z.W., Yang X.L., Li T.Z. (2019), *Face stability analysis of tunnels under steady unsaturated seepage conditions*, Tunnelling and Underground Space Technology, vol. 93, pp. 1-8.
- Lü X., Zhou Y., Huang M., Zeng S. (2018), *Experimental study of the face stability of shield tunnel in sands under seepage condition*, Tunnelling and Underground Space Technology, vol. 74, pp. 195-205.
- Marinos V., Marinos P., Hoek E. (2005), *The geological strength index : applications and limitations*, Bulletin of Engineering and Geological Environment, n°64, pp. 55-65.
- Messerli J., Pimentel E., Anagnostou G. (2010), *Experimental study into tunnel face collapse in sand*, Proceedings of the 7th International Conference in Physical Modelling in Geotechnics, Zurich, Switzerland.
- Mollon G., Dias D., Soubra A.H. (2011), *Rotational failure mechanisms for the face stability analysis of tunnels driven by a pressurized shield*, International Journal for Numerical and Analytical Methods in Geomechanics, vol 35, n°12, pp. 1363-1388.
- Mollon G., Dias D., Soubra A.H. (2013), *Continuous velocity fields for collapse and blowout of a pressurized tunnel face in purely cohesive soil*, International Journal for Numerical and Analytical Methods in Geomechanics, vol 37, n°13, pp. 2061-2083.
- NF EN 1997-1 (2005), *Eurocode 7 : Geotechnical Design – Part 1: General Rules*.
- NGI (2013), *Using the Q-system – Rock mass classification and support design*, Handbook of the Norwegian Geotechnical Institute, 57 p.
- Pan Q., Dias D. (2016), *The effect of pore water pressure on tunnel face stability*, International Journal for Numerical and Analytical Methods in Geomechanics, vol. 40, n°15. pp. ...
- Pan Q., Dias D. (2017), *Upper-bound analysis on the face stability of a non-circular tunnel*, Tunnelling and Underground Space Technology, vol. 62, pp. 96-102.
- Pan Q., Dias D. (2018), *Three dimensional face stability of a tunnel in weak rock masses subjected to seepage forces*, Tunnelling and Underground Space Technology, vol. 71, pp. 555-566.
- Paternesi A., Schweiger H.F., Ruggeri P., Fruzzetti V.M.E., Scarpelli G. (2017), *Comparisons of Eurocodes design approaches for numerical analysis of shallow tunnels*, Tunnelling and Underground Space Technology, vol. 62, pp. 115-125.
- Peila D. (1994), *A theoretical study of reinforcement influence on the stability of a tunnel face*, Geotechnical and Geological Engineering, n°12, pp. 145-168.
- Perazzelli P., Anagnostou G. (2017), *Analysis Method and Design Charts for Bolt Reinforcement of the Tunnel Face in purely Cohesive Soils*, J Geotech Geoenviron Eng 143 (9).
- Perazzelli P., Leone T. Anagnostou G. (2014), *Tunnel face stability under seepage flow conditions*, Tunnelling and Underground Space Technology, vol. 43, pp. 459-469.
- Piakowski A., Kowaleski Z. (1965), *Application of thixotropic clay suspensions for stability of vertical sides of deep trenches without strutting*, Proceedings of 6th International Conference on Soil Mechanics and Foundations Engineering, Montreal, vol. 111.

- Quarmout M., König D., Gussmann P., Thewes M., Schanz T. (2019), *Tunnel face stability analysis using Kinematical Element Method*, Tunnelling and Underground Space Technology, vol. 85, pp. 354-367.
- Salençon J. (1990), *An introduction to the yield design theory and its application to soil mechanics*, European Journal of Mechanics A-Solids, vol 9, n°5, pp. 477-500.
- Schofield AN. (1980), *Cambridge geotechnical centrifuge operations*, Geotechnique, vol. 30, n°3, pp. 227-268.
- Schuerch R., Poggiati R., Anagnostou G. (2019), *Design charts for estimating face stand-up time in soft ground tunnelling*, Proceedings of the World Tunnel Congress, Naples, 10 p.
- Senent S., Yi C., Jinenez R. (2020), *An upper bound solution for tunnel face stability analysis considering the free span*, Tunnelling and Underground Space Technology, vol. 103, pp. 1-14.
- Subrin D. (2002), *Études théoriques sur la stabilité et le comportement des tunnels renforcés par boulonnage*, thèse de doctorat de l'INSA de Lyon, 210 p.
- Toraldo C., Modoni G., Ochmanski M., Croce P. (2018), *The characteristic strength of jet-grouted material*, Géotechnique, vol. 68, n°3, pp. 262-279.
- Ukrichton B., Yingchaloenkitkhajorn K., Keawsawasvong S. (2017), *Three-dimensional undrained tunnel face stability in clay with a linearly increasing shear strength with depth*, Computers and Geotechnics, vol. 88, pp. 146-151.
- Vermeer P.A., Ruse N., Marcher T. (2002), *Tunnel heading stability in drained ground*, Tunnelling, Felsbau, vol. 20, n°6, pp. 8-18.
- Viana Da Fonseca A., Topa Gomes A. (2011), *A tunnel collapse on the construction in metro do Porto : solutions for optimization of advance control parameters of a EPB TBM*, Proceeding, of the XXV technical conference, Miedzydroje, 24-24 mai 2011.
- Vu M.N., Broere W., Bosch J. (2015), *The impact of shallow cover on stability when tunnelling in soft soils*, Tunnelling and Underground Space Technology, vol. 50, pp. 507-515.
- Wong H., Subrin D. (2006), *Stabilité frontale d'un tunnel : mécanisme 3D en forme de corne de rhinocéros et influence de la profondeur*, Revue européenne de génie civil, vol. 10, n°4, pp. 429-456.
- Xu T., Bezuijen A. (2018), *Analytical methods in predicting excess pore water pressure in front of slurry shield in saturated sandy ground*, Tunnelling and Underground Space Technology, vol. 73, pp. 203-211.
- Zapata Franco D., Janin J.P., Dano C., Le Bissonnais H., Falconi F., Gérardin C. (2020), *Méthodes 3D simplifiées pour évaluer l'impact du boulonnage au front : REX de la L11-GC03*, Paris, Journées Nationales de Géotechnique et de Géologie de l'Ingénieur, Lyon, 8 p.
- Zingg S., Anagnostou G. (2016), *An investigation into efficient drainage layouts for the stabilization of tunnel faces in homogeneous ground*, Tunnelling and Underground Space Technology, vol. 58, pp. 49-73.
- Zou J., Chen G., Qian Z. (2019a), *Tunnel face stability in cohesion-frictional soils considering the soil arching effect by improved failure models*, Computers and Geotechnics, vol. 106, pp. 1-17.
- Zou J.F., Qian Z.H., Xiang X.H., Chen G.H. (2019b), *Face stability of a tunnel excavated in saturated nonhomogeneous soils*, Tunnelling and Underground Space Technology, vol. 83, pp. 1-17.

APPENDIX: FACE STABILITY EXAMPLES

Some examples are presented in the following tables. If you have any additional examples, please send them in a similar format to ggd.cetu@developpement-durable.gouv.fr so that they can be included in a future update of this information document.

Tunnel name: Schirmeck (France)	
Tunnelling method: conventional	
<p>Year: 2004</p> <p>Nature of the ground: Transition zone between (i) a highly fractured rock facies, moderately altered, rather dry, and (ii) a second very highly fractured and completely altered facies, with fairly significant water inflows.</p> <p>Observations and adaptation of support methods: At PM 218, at the end of mucking, the face collapsed over almost its entire width according to a fracturing plane with a dip of around 45° in the direction of the tunnel. The total volume of the collapse was about 100 m³ (Figure a). Tunnelling continued after stabilising the face with 28 m³ of sprayed concrete and 30 4-meter long longitudinal expansive bolts. Given the precarious stability conditions observed, front bolting using 4-meter long longitudinal expansive bolts was systematically applied up to PM 465. This prevented the emergence of a new global instability mechanism, but local instabilities persisted, such as that at PM 235 visible in Figure (b).</p> <p>Overall implications for the project: The total duration of the boring and support work was about twice as long as expected. This is related in particular to the increase in the length of tunnel with steel arches (to the detriment of a bolted profile), naturally accompanied by a larger sprayed concrete thickness. The use of more face bolts also contributes to this, but this cannot be quantified precisely.</p>	 <p style="text-align: center;"><i>(a) Collapse of the face at PM 218.</i></p>  <p style="text-align: center;"><i>(b) Localised side wall collapse of the face at PM 235.</i></p>

Tunnel name: Bois de Peu (France)

Tunnelling method: conventional

Year: 2006

Nature of the ground:

Wet clays.

Observations:

Three major face collapses, with a volume of more than 50 m³, occurred at MP 518, 515 and 510 of the counter-boring of the descending tube under an overburden thickness of about ten meters. The fibreglass bolts, installed at the face with a density of 0.25 bolts per m², did not prevent the face instabilities, which did not, however, spread to the surface due to the umbrella vault initially installed.

Reinforcement and adaptations in methods:

Boring continued but was done in separate sections (top heading and bench) for about fifteen meters, until the shear strength of the ground improved.

Implications for the project:

Increase in the duration of the work by about 1 month, and an additional cost of about 500 k€ ex. tax according to the final general cost calculations for the works contract.



View of the face after one of the collapses. The face bolts as well as the umbrella vault are clearly visible. © Nicolas Dupriez, DDE 25.

Tunnel name: Porto (Portugal) metro

Tunnelling method: pressurized face TBM (earth pressure)

Year: 2001

Nature of the ground:

Mixed and heterogeneous face composed of unaltered granites in the lower part of the face, and highly altered granites in the upper part.

Observations:

Three local instabilities observed during the boring of the first 600 m of metro line C, including one leading to a sinkhole causing the collapse of a building and the death of a resident. This sinkhole appeared about 30 m after the passage of the face. This was caused by the over-excavation of the upper part of the face, linked to the contrast in the strength between unaltered and altered granites and by an initial difficulty (technical and organizational) in ensuring a full and pressurized chamber.

Reinforcement and adaptations in methods:

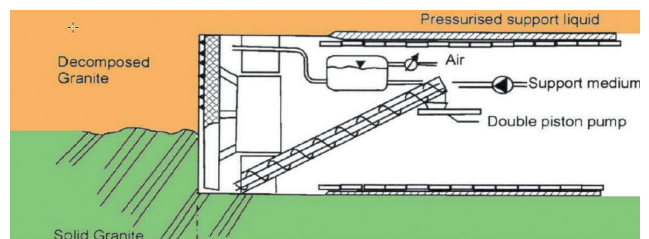
Following this accident, the conditioning was reviewed, construction crews were strengthened, monitoring procedures were revised, and the TAP (Tunnelling Advance Plan) for each 500 m section was introduced for the first time. In addition, a pressurized bentonite injection system was added to the TBM. This was triggered automatically when the pressure measured at the crown of the working chamber fell below a preset value. No other sinkholes were encountered during the remaining work on the C line and S line.

Implications for the project:

The death of a third party necessarily had a very negative impact on the start of this project. The corresponding financial consequences have not been published. The project was delayed by about 6 months.



(a) Sinkhole appeared on the surface.



(b) Longitudinal section illustrating the mixed face encountered, and the complementary system for injecting bentonite at the crown which was added following the collapse.

Reference : Grasso et al. (2003), Viana Da Fonseca & Topa Gomes (2011).

Tunnel name: Rennes metro (France)**Tunnelling method: pressurized face TBM (earth pressure balanced shield)****Year:** 2016**Nature of the ground:**

Shale, which was more or less altered.

Observations:

Several surface sinkholes were generated when boring this metro line. These include the one of about 20 m² and at least 3 m deep generated in the Noz store. These sinkholes are linked to the very particular structure of the rock mass, consisting of steeply inclined banks (70°), whose discontinuities tended to open and be lubricated under the effect of the confinement pressure.

Reinforcement and adaptations in methods:

During construction, a bentonite injection system (integrated bubble) was added to the tunnel boring machine, and monitoring of the confinement pressure was increased, ensuring that it was not too high.

Implications for the project:

The TBM was stopped for 133 days, costing an additional €10 million.



Photograph of the sinkhole that appeared in the Noz store. It has a surface area of about 20 m² and is 3 m deep. Three people fell into this sinkhole, but were able to get out of it without serious injury.

© Journal Ouest-France dated 2016/11/19.
Reference: tunnelling sheet for AFTES GT4 n°126, TES n°274.

Tunnel name: Nice metro (France)**Tunnelling method: pressurized face TBM (slurry shield)****Year:** 2017**Nature of the ground:**

Mixed subsidence composed of undulating ground (limestone and puddingstone) and soft ground (sand and pebbles).

Observations:

Several sinkholes developed on the surface, including one approximately 6 m in diameter and 1.5m in depth, in the middle of the rue de France. The latter did not cause any damage to the neighbouring buildings nor any traffic accident. This sinkhole was caused by the TBM encountering an old cavity filled with construction materials, notably steels stuck in the cutter head, with a loss of pressure in the working chamber.

Reinforcement and adaptations in methods:

Injections were carried out over fifteen meters around the sinkhole to improve the stability of the ground, then the cutter head was released, enabling tunnelling to be resumed.

Implications for the project:

Work stoppage of about 1.5 months.



Photograph of the sinkhole in Rue de France.

© Patrick Allemand.

Reference: Batiactu.com, 2017/07/05 and 2017/08/25.

Authors: Nicolas BERTHOZ, Didier SUBRIN.

Internal reviewers : Michel DEFFAYET, Eric PREMAT, Cédric GAILLARD, Gilles HAMAIDE, Johan KASPERSKI.

External reviewers : Denis BRANQUE (ENTPE), Martin CAHN (TERRASOL-SETEC), Guillaume CHAMPAGNE DE LABRIOLLE (ARCADIS), Elena CHIRIOTTI (INCAS PARTNERS), Fabrice EMERIAULT (Grenoble INP), Jean-Pierre JANIN (LOMBARDI INGENIERIE), Christophe JASSIONNESSE (SPIE BATIGNOLLES), Adrien SAITTA (EGIS TUNNELS).

Centre d'Études des Tunnels (Centre for Tunnel Studies)

25 Avenue François Mitterrand
69500, Bron, France
Tel. +33 (0)4 72 14 34 00
Fax. +33 (0)4 72 14 34 30
cetu@developpement-durable.gouv.fr

www.cetu.developpement-durable.gouv.fr



**MINISTÈRE
CHARGÉ
DES TRANSPORTS**

*Liberté
Égalité
Fraternité*

